

UNCLASSIFIED

AD NUMBER

AD480201

LIMITATION CHANGES

TO:

Approved for public release; distribution is unlimited. Document partially illegible.

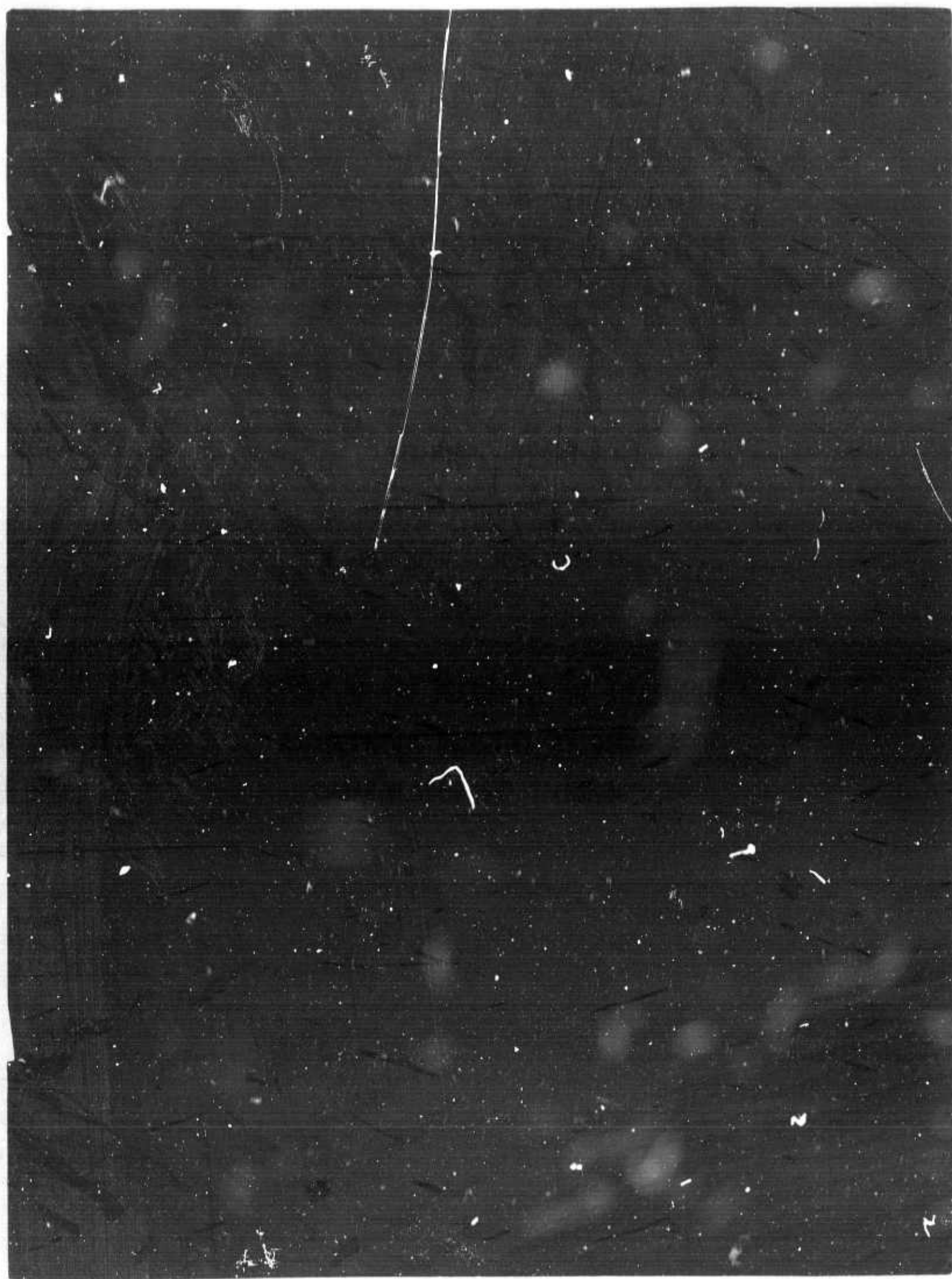
FROM:

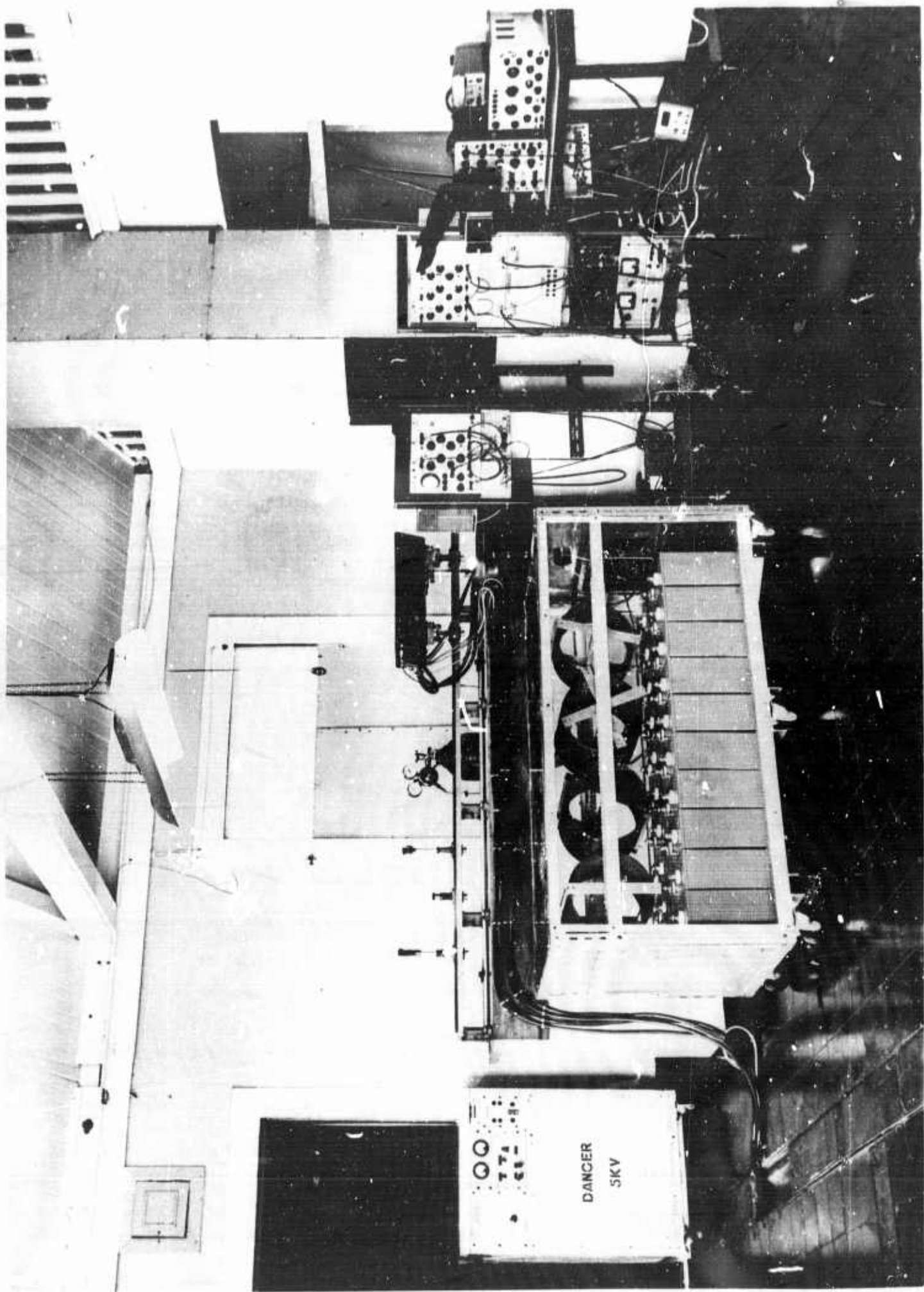
Distribution authorized to U.S. Gov't. agencies and their contractors;  
Administrative/Operational Use; MAY 1965. Other requests shall be referred to Air Force Office of Scientific Research, Arlington, VA. Document partially illegible.

AUTHORITY

AFCRL ltr 22 Dec 1971

THIS PAGE IS UNCLASSIFIED





Form 1473

AF - AFOSR - 616-64

11 May 1965,

12 72p.

JUSTIFY BELOW FOR	
OFSTI	NUMBER SUBMITTED TO
PROG	DATE RECEIVED
INSTRUCTIONS	
1473	
DATE OF REVIEW/ANNUALITY SCORE	
FILE	ANNUALITY OF ORIGINAL
2	

Annual  
Scientific Report.

April 1964 - March 1965,

6 A Study of the Feasibility of Measuring  
Atmospheric Densities by using a  
Laser - Searchlight Technique.

70 B.R. Clemesha, G.S. Kent, and R.W.H. Wright.

14 UWI - P2

DDC  
RECEIVED  
APR 7 1965  
RECEIVED  
A

De



# ABSTRACT

An analysis is made of the design of equipment to be used for measuring atmospheric densities by observing the scattering from a laser light-beam projected vertically into the atmosphere. This analysis is made in terms of both the expected scattering under typical conditions and the experimental difficulties which are encountered. A complete description is given of an equipment constructed to make such measurements and the early results are described. It is shown that the method works well with the comparatively simple apparatus used. Up to 30 Km. various dust and aerosol layers can be observed both by day and by night. Between 30 Km and 70 Km the variation of the atmospheric density with height can be measured at night and has been found to agree with values calculated on the basis of Rayleigh scattering and assuming a model atmosphere. The possible examination of meteoric dust at altitudes between 80 Km and 140 Km is discussed. The proposed future developments of the equipment are outlined.

## CONTENTS

1. Introduction
  2. Theoretical Considerations
    - 2.1 Rayleigh Scattering
    - 2.2 Particulate Scattering
    - 2.3 Experimental Design
    - 2.4 Other Workers Results
  3. The Experimental Techniques
    - 3.1 General Description of Receiver and Transmitter
    - 3.2 The Transmitter
    - 3.3 The Receiver
    - 3.4 The Alignment of the Receiver and Transmitter
  4. The Experimental Results
    - 4.1 Introduction
    - 4.2 Comparison with Rayleigh Scattering Theory
    - 4.3 The Dust Layers
    - 4.4 The Daytime Measurements
  5. Programme of Future Work
- References

## 1. INTRODUCTION

This report contains an account of a study, carried out in Kingston, Jamaica, between April 1st 1964 and March 31st 1965, of the feasibility of measuring atmospheric density by a laser-searchlight technique. The method is essentially an optical radar, using a pulsed ruby laser as a transmitter and an astronomical telescope as receiver. Light from the transmitted pulse is scattered by atmospheric molecules and by any other particles in the atmosphere, and measurements are made on the amount of scattered radiation received on the ground from different altitudes. In the absence of other scattering centres, such as water droplets and dust particles, the intensity of the scattered signal may be used to deduce the molecular density.

Elterman (1951), working in New Mexico, observed the scattering from a modulated search-light beam and obtained a measurement of the atmospheric density to an altitude of about 60 kilometres. Since then he has made numerous measurements up to this height and obtained information on the temperature profile at different seasons (Elterman, 1954). More recently (Elterman and Campbell, 1964) the same technique has been used to study the properties of the aerosol layer at a height of about twenty kilometres.

The discovery of the ruby laser has led to the substitution of this for the searchlight with a number of advantages. The energy from the laser is produced in a short very high energy pulse. This enables the transmitter and receiver to be placed together and the scattered power returned from any range to be found in a manner exactly analogous

to the conventional radar: this is not at present possible using a searchlight. The narrow frequency spread and the small angular divergence of the transmitted beam allow the noise caused by the background brightness of the night sky to be reduced to negligible proportions. In fact, as will be shown later, observations can be made to a considerable altitude even during the day. This method has been used by Fiocco and Colombo (1964) to observe echoes which they attribute to dust layers at altitudes between 70 and 140 kilometres.

The remainder of this report contains a description of the construction and testing, in Kingston, Jamaica, of such an optical radar system and some initial measurements made with it. This equipment has a considerably greater sensitivity than that obtained by other workers in this field and, when fully operational, will enable measurements to be made quickly and at frequent intervals up to heights of about 80 kilometres. In Section 2. the theory of molecular scattering is discussed together with an outline of that expected from dust and aerosol particles. A discussion of some of the special experimental problems which arise is also made, together with a summary of measurements already made by other workers. In Section 3. the construction and operation of the radar system is described in a certain amount of detail, this having been the major part of the work carried out this year. In Sections 4. and 5. the results already obtained are described. A survey is then made of the developments and further experiments which it is hoped will be carried out during the coming year.

## 2. THEORETICAL CONSIDERATIONS

### 2.1 Rayleigh Scattering

The theory of scattering from molecules was first developed by Rayleigh (1871) and is discussed in the context of general scattering theory by Van de Hulst (1957). The results of the theory may be summarised as follows.

Let a plane wave of intensity  $I_0$  be incident on a gas containing  $n$  molecules per unit volume, whose polarisability is  $\alpha$ . Then it may be shown that the scattered intensity, at a distance  $r$ , in a direction  $\theta$ , as shown in Fig.1(a) is given by

$$\text{either (1) } I = \frac{k^4}{r^2} |\alpha|^2 V I_0 n$$

$$\text{or (2) } I = \frac{k^4}{r^2} \cos^2 \theta |\alpha|^2 V I_0 n$$

In these equations  $k = \frac{2\pi}{\lambda}$ , where  $\lambda$  is the wavelength, and  $V$  is the scattering volume.

(1) refers to the case of the electric vector in the incident wave being perpendicular to the plane containing the incident and scattered waves, and

(2) to the case in which the vector is parallel.

For back-scatter, no distinction between these cases arises and

$$I = \frac{k^4}{r^2} |\alpha|^2 V I_0 n$$



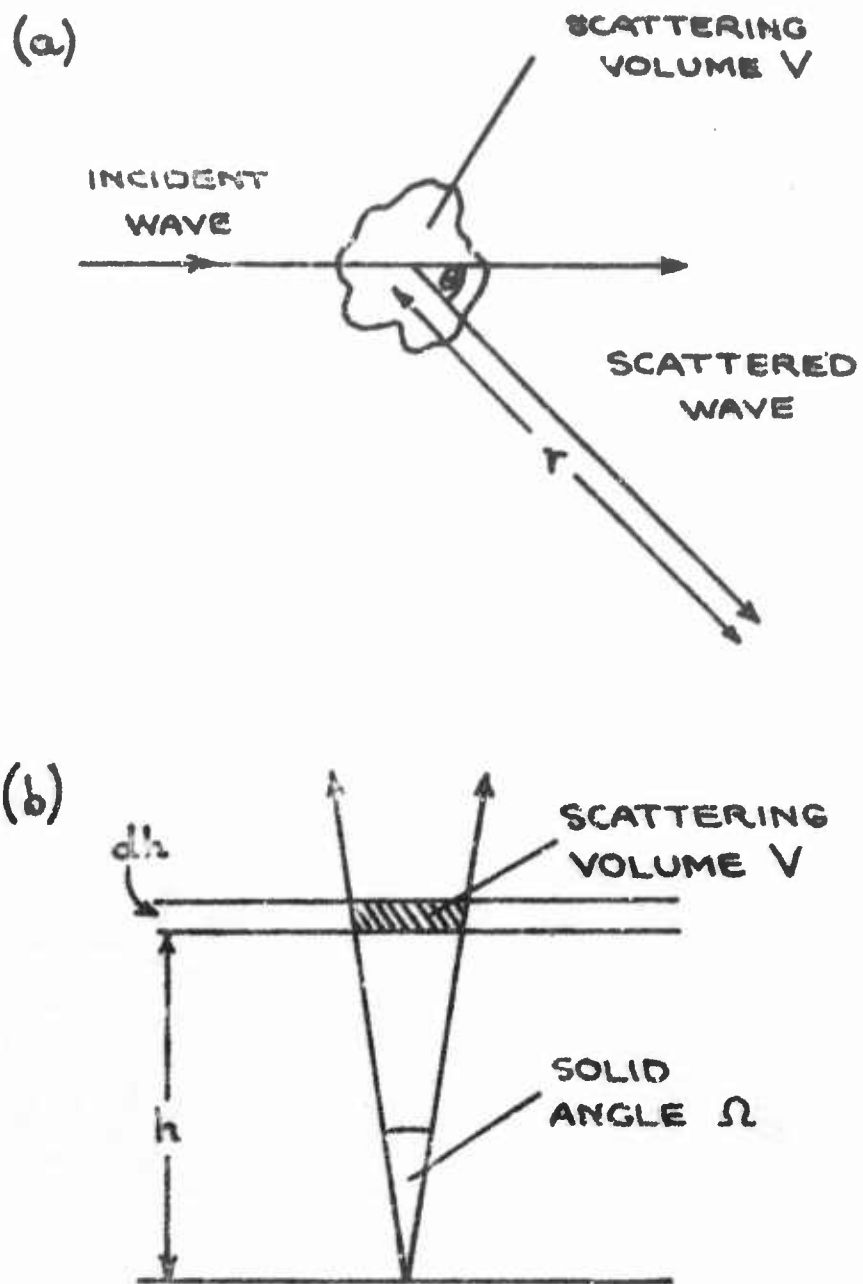


FIG. 1 THE SCATTERING GEOMETRY

$$= \frac{16 \pi^4}{\lambda^4 r^2} |\alpha|^2 V I_0 n$$

The polarisability  $\alpha$  is related to the refractive index  $\mu$  by the formula

$$2 \pi \alpha = (\mu - 1)/n$$

$(\mu - 1)/n$  has the value  $1.08 \times 10^{-23} \text{ cm}^3$  for light in the visible region of the spectrum

We have therefore 
$$I = \frac{4 \pi^2 (\mu - 1)^2}{\lambda^4 r^2 n^2} V \cdot n \cdot I_0$$

Rayleigh scattering is frequently described in terms of various scattering cross-sections and considerable confusion can arise. The following are in common use.

#### 1) The Rayleigh Scattering Cross-section

$$\rho_r = \frac{32 \pi^3 (\mu - 1)^2}{3 \lambda^4 n^2}$$

The total fraction of light scattered per unit path length from a beam traversing a region with  $n$  molecules per unit volume is

$$\rho_r \cdot n$$

This formula may be obtained by integrating the general formulae for  $I$ , given earlier, over a complete sphere.

#### 2) The Rayleigh Scattering Function for Back-scatter

$$\rho_R = \frac{4 \pi^2 (\mu - 1)^2}{n^2 \lambda^4} = \frac{3}{8 n} \rho_r$$

The fraction of light back-scattered, per unit path length, per unit solid angle, from an incident beam is

$$\rho_R \cdot n$$

### 3) The Radar Cross-section

$$\rho = \frac{16 \pi^3 (\mu - 1)^2}{n^2 \lambda^4} = 4 \pi \rho_R = \frac{3}{2} \rho_r$$

The fraction of light that would be scattered per unit length, from an incident beam, if the amount of scatter in all directions were the same as that for back-scatter, is

$$\rho \cdot n$$

In most publications on back-scattering either  $\rho_R$  or  $\rho$  is used. We may rewrite the formula for  $I$  as

$$I = \frac{\rho_R \cdot V \cdot n \cdot I_0}{r^2}$$

where  $\rho_R$  has the numerical value of  $1.98 \times 10^{-28} \text{ cm}^2 \text{ sterad}^{-1}$  at a wavelength of  $6943 \text{ \AA}$ .

Consider a pulse of length  $t$  seconds, containing  $N_0$  photons, which is directed upwards through the lower atmosphere. Let the attenuation in passing through the lower atmosphere be  $T$ , then the intensity at a height  $h$  is

$$\frac{N_0 T}{t h^2 \Omega} \quad \text{photons per unit area per unit time}$$

where  $\Omega$  is the angular beamwidth. If we consider the scattering from a thin slice of height  $dh$ , as shown in Fig.1(b) then

$$V = h^2 \Omega \, dh$$

and the scattered intensity at the ground is

$$\frac{\rho_R \cdot N_0 \cdot T^2 n \, dh}{t h^2}$$

Because of the length of the transmitted pulse, light will be received simultaneously from a height range  $ct/2$ , where  $c$  is the velocity of light. So the total intensity on the ground is

$$\frac{\rho_R N_0 T^2 n \cdot c}{2h^2}$$

provided  $ct/2$  is small compared with the scale of variation of  $n$ .

If we integrate for a time  $\tau$ , the amount of light collected on a mirror of diameter  $D$ , then the number of collected photons will be

$$N = \frac{\pi D^2 \tau \rho_R N_0 T^2 n c}{8 h^2}$$

If the light is then allowed to fall onto a photomultiplier whose quantum efficiency is  $Q$  then the number of photons actually recorded is

$$C = \frac{n \rho_R}{h^2} \cdot \frac{\pi D^2 \tau c N_0 T^2 Q}{8}$$

In order to obtain estimates for the scattering cross-sections and the number of expected photons, values of  $n$  have been calculated using the modified U.S. standard atmosphere for  $^{15}\text{N}$  (Cole and Kantor, 1963). These are shown in Table I together all three scattering cross-sections calculated at 10 kilometre height intervals. In order to obtain an estimate of  $C$  various assumptions have to be made about the experimental parameters. These have been taken to be

$$D = 50 \text{ cms.}$$

$$\tau = 10^{-5} \text{ second (corresponding to a height interval of 1.5 kilometres).}$$

$$C = 3 \times 10^{16} \text{ cm}^{-3} \text{ sec}^{-1}$$

$$N_0 = 1.75 \times 10^{19} \text{ (the number of photons in a five joule pulse at } 6943 \text{ } \overset{\circ}{\text{A}}.)$$

$$T^2 = 0.5$$

$$Q = 0.03$$

In these figures the two most unreliable are those for the total transmitted power and the attenuation in the lower atmosphere. The former is based on measurements made on the power in the laser beam and these will be discussed later in the section on experimental techniques. The latter is taken from a model proposed by Elterman (1964) for attenuation in the lower atmosphere. As nearly all the attenuation occurs in the bottom two or three kilometres and consequently depends very much on local conditions, it could be very seriously in error.

Taking these constants

$$\frac{\pi D^2 \tau c N_0 T^2 Q}{8} = 7.73 \times 10^{25} \text{ cm}^3$$

and the resultant values for  $C$  are those shown in the final column in Table I. These figures must be taken as maximum values. Reflection losses occur in any system and, as will be explained in Section 2.3, we find it necessary to employ narrow band filters which transmit about 50% of the light falling on them. It can be seen from the figures that, taking into account the system losses, above about 55 kilometres less than one recorded photon is obtained for each output pulse. This situation may be improved slightly by increasing



TABLE I

h Kms.	$n$ $\text{cm}^{-3}$	$n \rho_R$ $\text{cm}^{-1} \text{ str}^{-1}$	$n \rho = 4\pi n \rho_R$ $\text{cm}^{-1}$	$n \rho_r = \frac{2}{3} n \rho$ $\text{cm}^{-1}$	$n/h^2$ $\text{cm}^{-5}$	$\frac{n \rho_R}{h^2}$ $\text{cm}^{-3} \text{ str}^{-1}$	C
10	$8.6 \times 10^{18}$	$1.70 \times 10^{-9}$	$2.14 \times 10^{-8}$	$1.43 \times 10^{-8}$	$8.6 \times 10^6$	$1.70 \times 10^{-21}$	$1.31 \times 10^5$
20	$2.0 \times 10^{18}$	$4.0 \times 10^{-10}$	$5.0 \times 10^{-9}$	$3.3 \times 10^{-9}$	$5.0 \times 10^5$	$9.9 \times 10^{-23}$	$7.7 \times 10^3$
30	$3.8 \times 10^{17}$	$7.5 \times 10^{-11}$	$9.4 \times 10^{-10}$	$6.2 \times 10^{-10}$	$4.2 \times 10^4$	$8.3 \times 10^{-24}$	$6.4 \times 10^2$
40	$8.6 \times 10^{16}$	$1.70 \times 10^{-11}$	$2.1 \times 10^{-10}$	$1.41 \times 10^{-10}$	$5.4 \times 10^3$	$1.07 \times 10^{-24}$	$8.3 \times 10$
50	$2.4 \times 10^{16}$	$4.8 \times 10^{-12}$	$6.0 \times 10^{-11}$	$4.0 \times 10^{-11}$	$9.6 \times 10^2$	$1.90 \times 10^{-25}$	$1.46 \times 10$
60	$6.7 \times 10^{15}$	$1.33 \times 10^{-12}$	$1.67 \times 10^{-11}$	$1.11 \times 10^{-11}$	$1.86 \times 10^2$	$3.7 \times 10^{-26}$	2.9
70	$1.88 \times 10^{15}$	$3.7 \times 10^{-13}$	$4.7 \times 10^{-12}$	$3.1 \times 10^{-12}$	$3.8 \times 10$	$7.5 \times 10^{-27}$	$5.8 \times 10^{-1}$
80	$4.4 \times 10^{14}$	$8.7 \times 10^{-14}$	$1.09 \times 10^{-12}$	$7.2 \times 10^{-12}$	6.9	$1.37 \times 10^{-27}$	$1.06 \times 10^{-1}$
90	$7.3 \times 10^{13}$	$1.45 \times 10^{-14}$	$1.82 \times 10^{-13}$	$1.21 \times 10^{-13}$	$9.0 \times 10^{-1}$	$1.78 \times 10^{-28}$	$1.38 \times 10^{-2}$

Rayleigh Scattering Parameters for a Standard Atmosphere.

(h is the altitude, n is the number density of molecules,  $n \rho_R$  is the Rayleigh Scattering Function at the given altitude,  $n \rho_r$  is the Rayleigh Scattering Cross-section,  $n/h^2$  and  $n \rho_R/h^2$  are functions used in the calculation of C, C is the expected count for the experimental parameters given in the text.)

the gating interval; the limit to this is really set by the scale height in the atmosphere and cannot usefully be made much more than 5 kilometres. The figure of one and one half kilometres was chosen above as this corresponds to the actual interval used in the recording system. A comparison of Table I with the actual signal observed will be made in Section 4.2.

In the above calculations the assumption has been made that the polarisability of the molecules is isotropic, from which it follows that the back-scattered wave is plane polarised in the same sense as the incident wave. This assumption is not completely true but it appears that the amount of depolarisation should not be more than a few per cent. (Van de Hulst, 1957).

## 2.2 Particulate Scattering

It is well known that the lower atmosphere contains suspended solid and liquid particles (aerosols) in large numbers. These vary in size from about one hundredth to one micron. (Junge 1963). The main characteristics of their variation with height are fairly well known up as far as about thirty kilometres (Junge and Manson, 1961; Junge, Chagnon and Manson, 1961; Rosen, 1964). An outline of this variation, as measured by balloon borne particle counters, is shown in Fig.2. It may be seen that there is a maximum near the ground followed by a further maximum near the tropopause. As the height of the tropopause varies considerably with latitude it is to be expected that the aerosol distribution will show a similar variation. The theory of the scattering (Mie scattering) from these aerosols is complex, the

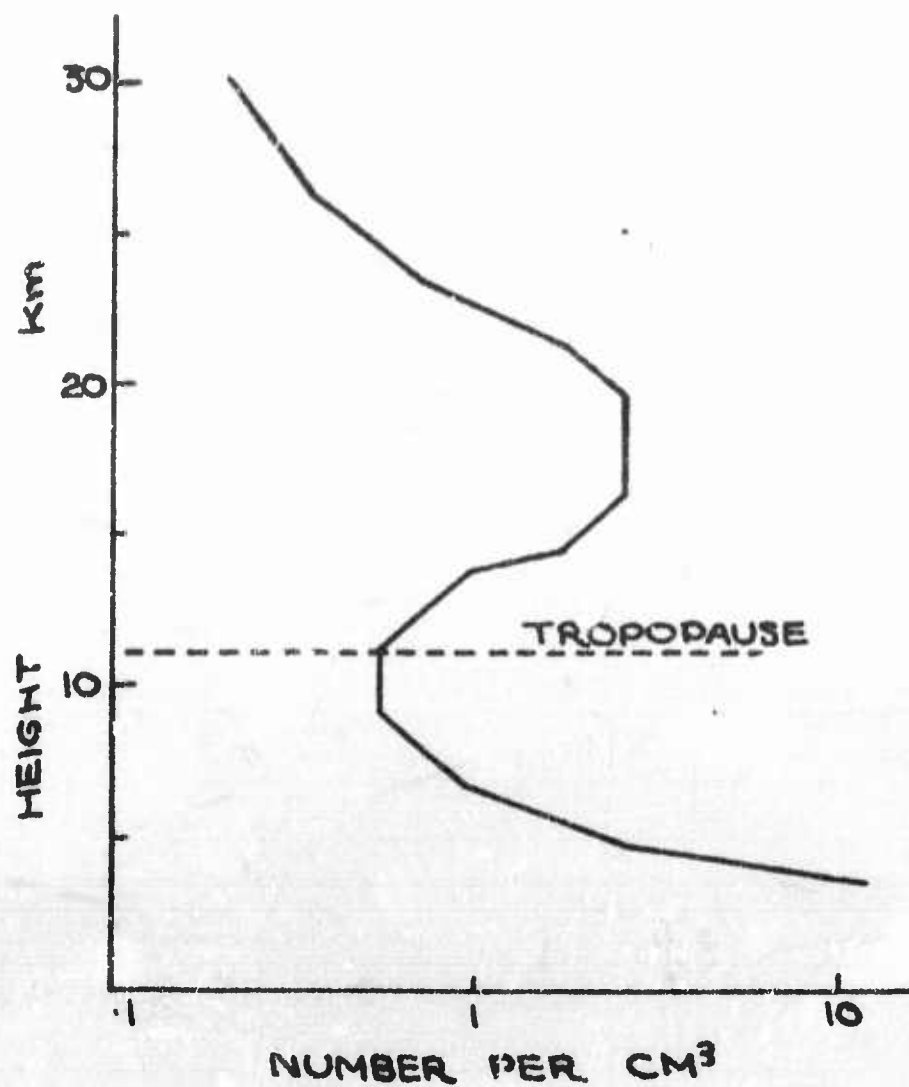


FIG.2. SCHEMATIC DIAGRAM SHOWING THE VARIATION OF AEROSOL NUMBER DENSITY WITH ALTITUDE FOR A TEMPERATE LATITUDE. (A COMPOSITE PICTURE TAKEN FROM SOURCES QUOTED IN THE TEXT).

scattering cross-section of a particle depending on the ratio of its diameter to the wavelength employed, its shape and the dielectric constant. Estimates, based on the known concentration of aerosol particles at twenty kilometres, indicate that the total amount of scattering expected from that level might be 20 - 30% above that due to scattering from the air molecules only. (Deirmendjian, 1965). Some observations made by the searchlight probing technique show an increase of about 50% and also indicate that the layer is bifurcated, with one maximum near the tropopause and one about seven kilometres higher (Elterman and Campbell, 1964).

The situation above thirty kilometres is far from clear. In papers which will be discussed later Fiocco and Smullin (1963) and Fiocco and Colombo (1964) have reported the existence of dust layers at heights of 60 - 90 kilometres and 110 - 140 kilometres. These layers they attribute to the fragmentation of meteoroids; the size of the fragments and the level at which the process would occur is however subject to a great deal of uncertainty. The theory of scattering in the mesosphere is discussed by Palmer and Zdunkowski (1964), who give graphs showing the concentration of particles necessary for the Mie scattering from them to be equal to the Rayleigh scattering at an altitude of 80 kilometres. These are given for a number of different sizes of both ice and silicate particles. Since the absolute rates of influx of meteoroids are very uncertain it is impossible to estimate from their curves what amount of scattering is to be expected. Actual laser observations on these altitudes should however make it possible

to reverse the theory and determine the particle concentration.

Very little appears in the papers quoted above on the polarisation of the scattered signal. Anisotropy in the shape of the scattering particles is almost certain to occur and this would be reflected in terms of depolarisation of the back-scattered signal. It appears (Van de Hulst, 1957) that this depolarisation would not normally be greatly in excess of that for neutral particles. It does however depend rather strongly on the dielectric constant and, in special cases, such as that of scattering from elliptical water particles, could be as high as 20%.

### 2.3 Experimental Design

The experimental measurement of the scattered signal has two main problems to contend with:

- i) to obtain enough signal to measure;
- ii) to reduce the background noise to a level well below the signal.

In the formulae developed in the last section the intensity of the scattered signal is proportional to  $N_0 D^2 \tau$  where  $N_0$  is the radiated power,  $D$  is the diameter of the receiving mirror and  $\tau$  is the period of integration.  $N_0$  and  $D$  should be made as large as possible consistent with the available funds:  $\tau$  is limited to about forty micro-seconds as explained earlier. In a practical system losses occur due to scattering and reflection from lenses and, to the less than perfect reflectivities obtainable with mirrored surfaces. These may be reduced, in the case of small components, by having them coated with dielectric reflecting or antireflecting layers and this has been done



with the majority of the surfaces used in our equipment. In the case of the large mirrors, the losses which occur in aluminised or silvered reflecting surfaces must be accepted. Further small losses will occur because the laser beam is not perfectly circular in shape and because it is desirable to reduce this to a circular beam containing perhaps 90% of the energy. Further discussion of these points will be made later in Section 4.2 when the intensity of the received signal is compared to the theoretical values.

One factor which reduces the received signal strength is absorption in the lower atmosphere. The presence of condensed water in the form of cloud or fog will clearly prevent the beam from reaching the upper atmosphere, but it is less obvious that water vapour itself may be a problem. The absorption spectrum of water vapour contains several maxima in the visible spectrum (Long, 1963) and, in particular, there is a line at  $6943.8 \text{ \AA}$ . This is very close to the normal output wavelength of the ruby laser which, in addition, is fairly strongly temperature dependent. It has been suggested (Hirono, 1964) that thermal tuning of the laser and measurement of the absorption might be a useful technique with which to measure the water vapour content of the atmosphere. It also follows that if the temperature of the laser alters without one's knowledge, this may cause a rather puzzling decrease in returned signal. This point is further discussed in the section on techniques.

Apart from these considerations, very little can be done to improve the amplitude of the received signal. One further point may

be made here however: in a system which counts pulses received in a given time interval there is likely to be a dead time between intervals. Our equipment is no exception to this, and, with the type of display used at the moment, this amounts to about 40% of the total. This is unfortunate and will be reduced in the future.

The subject of background noise is not so simple as that of signal strength. Noise will arise from the following sources -

- i) the sky background
- ii) the photomultiplier
- iii) other sources of weak radiation at  $6943 \text{ \AA}$  such as fluorescence.

The noise associated with the sky brightness is by no means uniform over the visible spectrum but it is essentially wide-band as compared to the single wavelength output of the laser. It might therefore be considered that the use of a narrow-band interference filter would be sufficient to reduce the sky-noise to a negligible level, while still passing the scattered light at  $6943 \text{ \AA}$ . In fact it would be possible on these grounds to work even during the day. In practice the situation is not quite so favourable. As the band-width of an interference filter is reduced so is the transmission at the central frequency. For a  $20 \text{ \AA}$  wide filter this amounts to about 60%; with a  $4 \text{ \AA}$  wide filter it is about 40% and decreases rapidly as the bandwidth is reduced below this. In addition the pass-band is sensitive to temperature changes. This might not normally be a serious problem but, as will be explained later, it is necessary to cool the photomultiplier and it may be difficult under these circumstances to maintain the filter temperature constant

to  $1^{\circ} - 2^{\circ}\text{C}$ . The other factor influencing the amount of sky background noise is the area of sky seen by the receiving mirror. This, in the ideal system corresponds to the angular beamwidth of the transmitted beam. This, in turn, is determined by the angular beamwidth of the laser and the characteristics of the optical system used to collimate it. As shown in Fig. 3. this consists of a diverging lens and a parabolic mirror. If the laser angular beamwidth is  $\alpha$  then the width of the transmitted beam is  $\alpha(\frac{d}{D})$  where  $D$  is the diameter of the transmitter mirror and  $d$  is the diameter of the laser beam. It is clear that  $D$  should be as large as possible. At the same time some attention must be paid to the receiving mirror, this has to be of sufficiently good quality to be able to resolve the transmitted beam. In practice this turns out to be a good deal less stringent a requirement than those for a good quality astronomical mirror. Using an eight inch transmitting mirror and a  $20 \text{ \AA}$  wide filter the light from the night sky is found to be negligible (figures are given in Section 3.3). During the day the background is very much higher but even so, using a  $4 \text{ \AA}$  filter, it is found to be less than the scattered signal at heights below 30 km. This height may be raised by about ten kilometres by doubling the diameter of the transmitting mirror and it is hoped eventually to do this in our system.

The next most important contribution to the noise is that due to fluorescence of the laser. This is the spontaneous emission of the  $6943 \text{ \AA}$  radiation from the ruby rod which is in contrast to the stimulated emission responsible for the laser output pulse. The

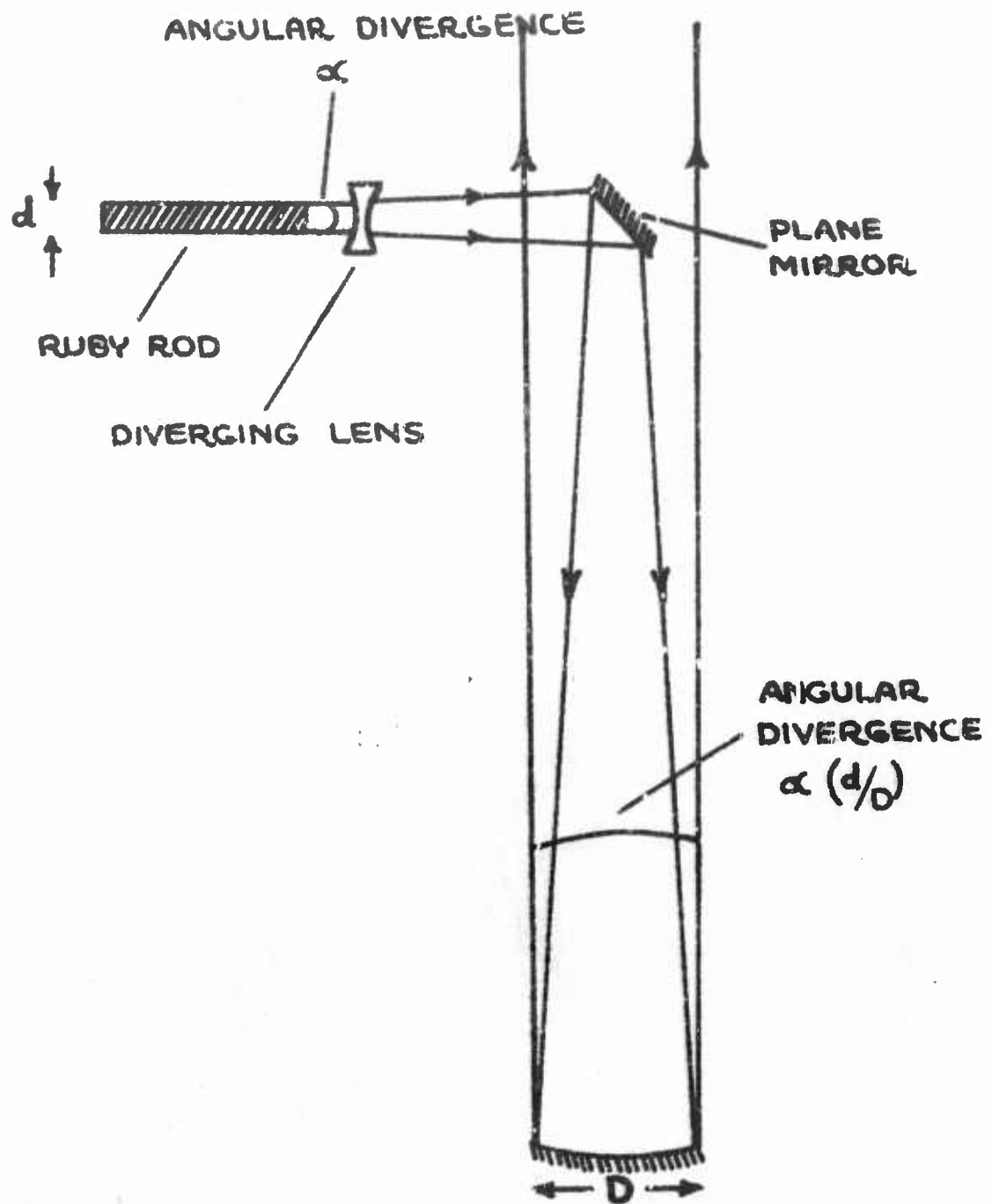


**FIG. 3** SCHEMATIC DIAGRAM OF THE OPTICAL TRANSMITTING SYSTEM.

fluorescence is very much weaker than the main laser pulse but persists for about two milli-seconds. Scattering of this from the lower atmosphere can result in a signal as strong as that scattered from the main pulse at great heights. Being of exactly the same frequency, the use of filters will not help discriminate against this. To eliminate the fluorescence a special shutter is required and the design of this is described in the section on experimental techniques.

Photomultiplier noise is considerable but fortunately may be reduced to negligible proportions by lowering the temperature of the photo-cathode. Details of this are also explained in Section 3.3. Various other minor sources of noise may be present which are appreciable when measuring the signal scattered from great altitudes. Those occurring with our equipment are still under investigation at the time of writing this report. They appear to be due either to fluorescence of one of the optical components used in the transmitter system or else of the lower atmosphere.

#### 2.4 Other Workers Results

Several groups of research workers are working on the problem of laser probing of the upper atmosphere but so far only Fiocco and his co-workers have published results. (Fiocco and Smullins, 1964; Fiocco and Colombo, 1964; Fiocco and Grams, 1964). Using a half-joule laser pulse with a 30 cm. diameter receiving mirror they have succeeded in detecting scattering from the neutral atmosphere up to about 60 km. The variation of the amount of scattering with height agrees quite well with the general accepted picture of the density



distribution. In addition they have observed the 20 kilometre aerosol layer, obtaining results similar to Elterman but with a rather greater enhancement of the layer and not showing the bifurcation. As mentioned earlier, they obtained echoes from between 70 and 140 km. considerably in excess of those expected from the neutral atmosphere. These are attributed to scattering from meteoroid fragments. A more detailed discussion of these results and a comparison to our own will be made in Sections 4.2. and 4.3.

### 3. THE EXPERIMENTAL TECHNIQUES

#### 3.1. General Description of Receiver and Transmitter

A photograph of the equipment is shown in the illustration at the beginning of this report and the assembly is shown schematically in Fig.4. Table 2. lists the equipment parameters. It may be conveniently divided into a transmitter and receiver. The transmitter consists of the laser, its power supply and the associated optics; the receiver consists of a large telescope mirror used in conjunction with a sensitive photomultiplier, an amplifier and a display unit. The laser itself is a Q-spoiled ruby laser capable of giving out a series of pulses within an interval of about 5 microseconds with a total energy content of about 5 joules. This is energised by discharging a 2000 $\mu$ F, 3 Kilovolt capacitor bank through two flash tubes in series and triggered with a pulse initially derived from the Q-spoiler. The beam from the laser passes through a rotating shutter, which cuts out the fluorescence, and is collimated, as explained earlier, via a diverging lens and a 20 cm. parabolic mirror. This gives a vertical beam with an angular spread of rather less than 0.4 milliradian.

The receiver consists of a 50 cm. telescope mirror used in the form of a vertical Newtonian telescope. At the focus of this mirror there is a narrow circular aperture to limit its field of view to the area of sky illuminated by the laser and the beam is then rendered parallel before falling on the photomultiplier. Provision is made for the insertion into the beam of neutral, polarizing, and narrow-band filters. The output from the photomultiplier is amplified and displayed in raster form on the face of an oscilloscope, where it is photographed.

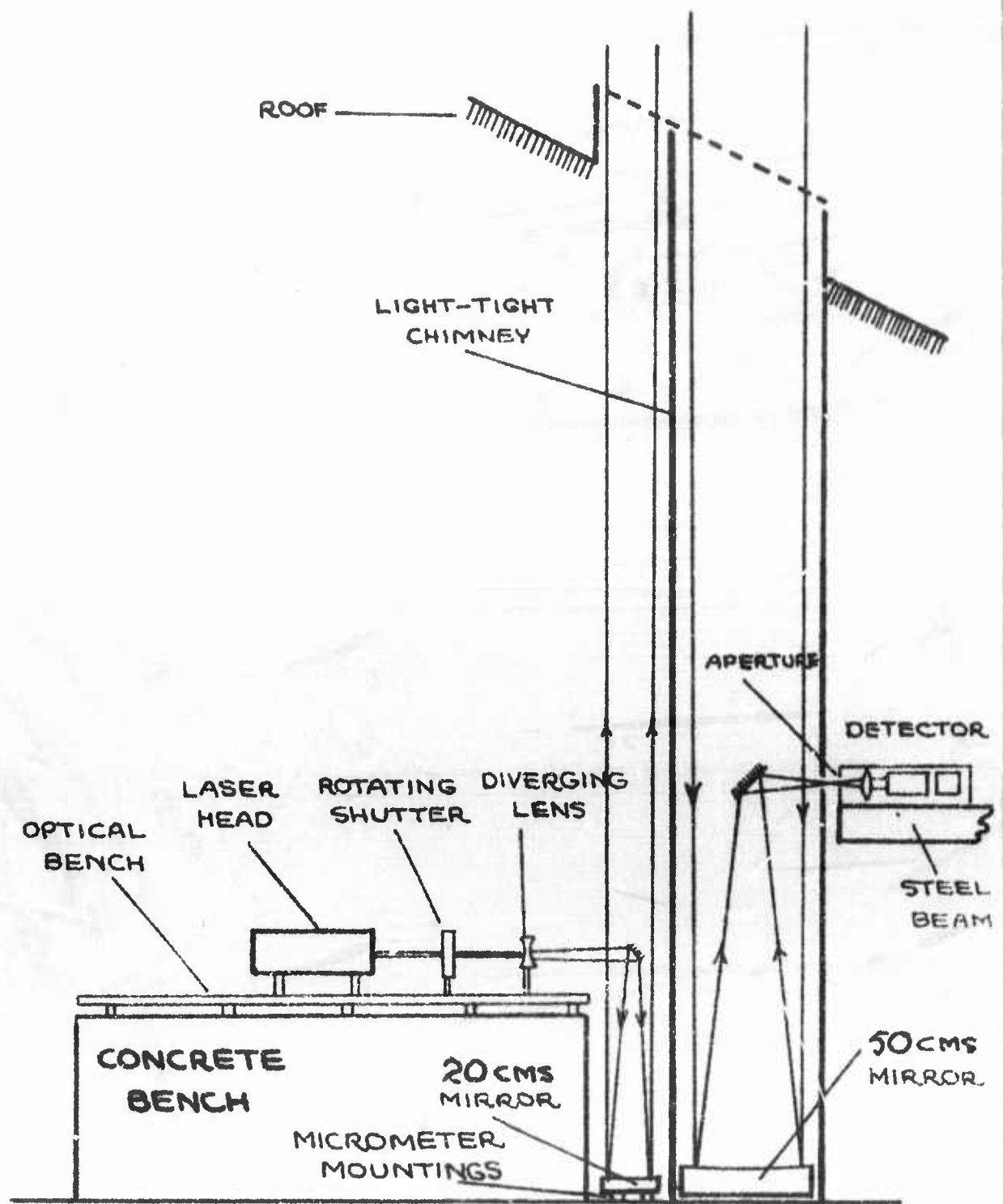


FIG.4 APPROXIMATE ARRANGEMENT OF THE TRANSMITTING AND RECEIVING SYSTEMS.

TABLE 2Characteristics of the Optical Radar System

Wavelength	6943 Å
Pulse length	<5 μ-seconds
Pulse energy	5 joules
Pulse repetition rate	<0.2 second <sup>-1</sup>
Transmitted beamwidth	<0.4 milliradian
Receiving aperture	0.21 metres <sup>2</sup>
Bandwidth of filters	20 Å and 4 Å
Quantum efficiency of photomultiplier	3%
Filter Transmissivities	60% (20 Å) and 40% (4 Å)

As may be seen in the illustration, the whole assembly is extremely rigidly mounted, the laser being on a good quality optical bench on top of a concrete base. The telescope mirror rests on the floor of the laboratory and the photomultiplier is mounted on a steel beam set into the laboratory walls. The transmitter and receiving systems are shielded from one another so that no light may pass directly from the former to the latter and there are adjustments on the transmitting mirror for collimating the two beams. The remaining equipment visible in the illustration is the capacitor bank, the five kilovolt power supply for charging this and the associated electronic equipment necessary for the control of the system and the detection and recording of the signal.

### 3.2 The Transmitter

A block diagram of the transmitting system is shown in Fig.5.

#### The Power Supply and Capacitor Bank

The power supply, which was constructed to charge the capacitor bank, which is in turn discharged through the flash-tubes in the laser, is capable of giving a 5 kilovolt peak output voltage at a mean rating of 5 kilowatts. The circuit used is shown in Fig.6. Avalanche diode rectifiers  $D$  are used in the main rectifying circuit. The current through these is limited by means of the resistance  $R$  included for simplicity in the primary circuit. These are forced air-cooled and may be used to vary the mean primary current between 6 and 20 amps. The choke  $L$  is included to prevent any negative pulse from the capacity bank damaging the rectifiers.

Fig. 7. shows the control circuits for voltage to which the capacitor bank is charged. A predetermined voltage between 1000 and 3000 volts may be selected and relay  $R_1$  opens at this value and prevents further charging. Should this circuit fail an identical safety control circuit, operating a different switch, will take over and prevent damage to the capacitor bank.

The charging rate of the power supply is limited by the current rating of the transformer and the rectifiers. Because of this the maximum secondary current is about one amp enabling the capacitor bank to be charged to its maximum working voltage of 3000 volts in about six seconds.

The capacitor bank contains 2000 $\mu$ F in 100 $\mu$ F units, rated at 3000 volts and designed for a discharge rate of 10 per minute. The condensers

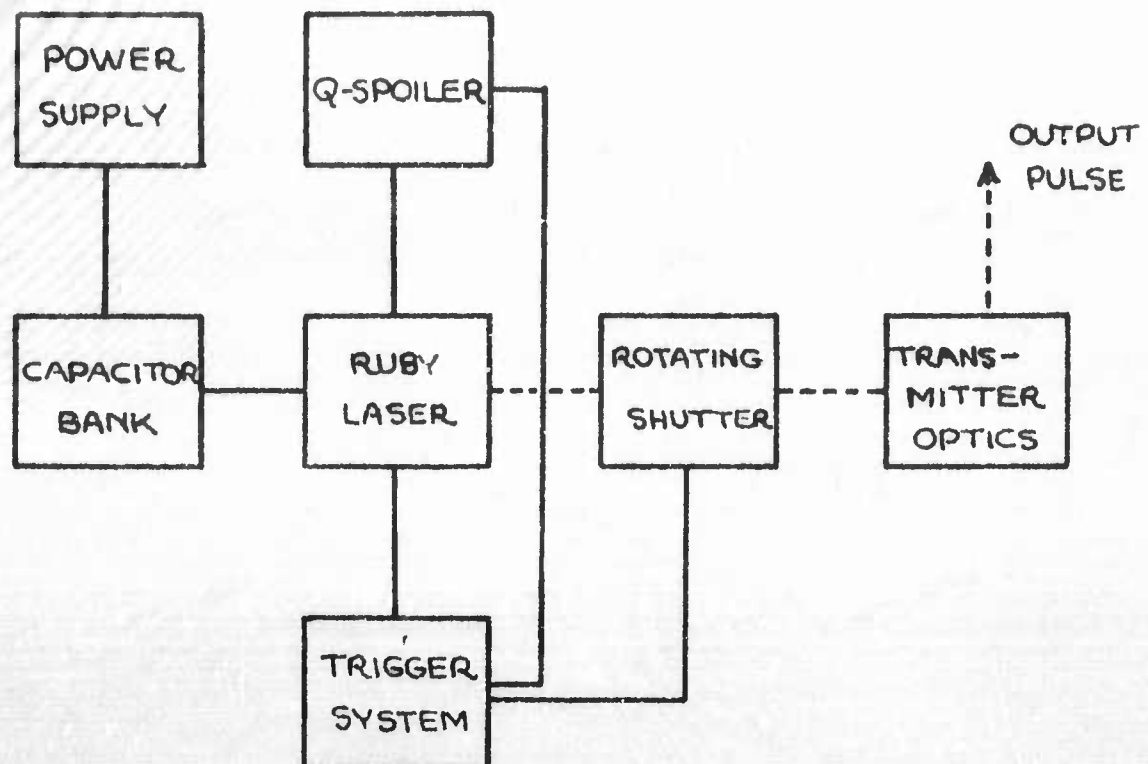


FIG. 5 BLOCK DIAGRAM OF THE TRANSMITTING SYSTEM.



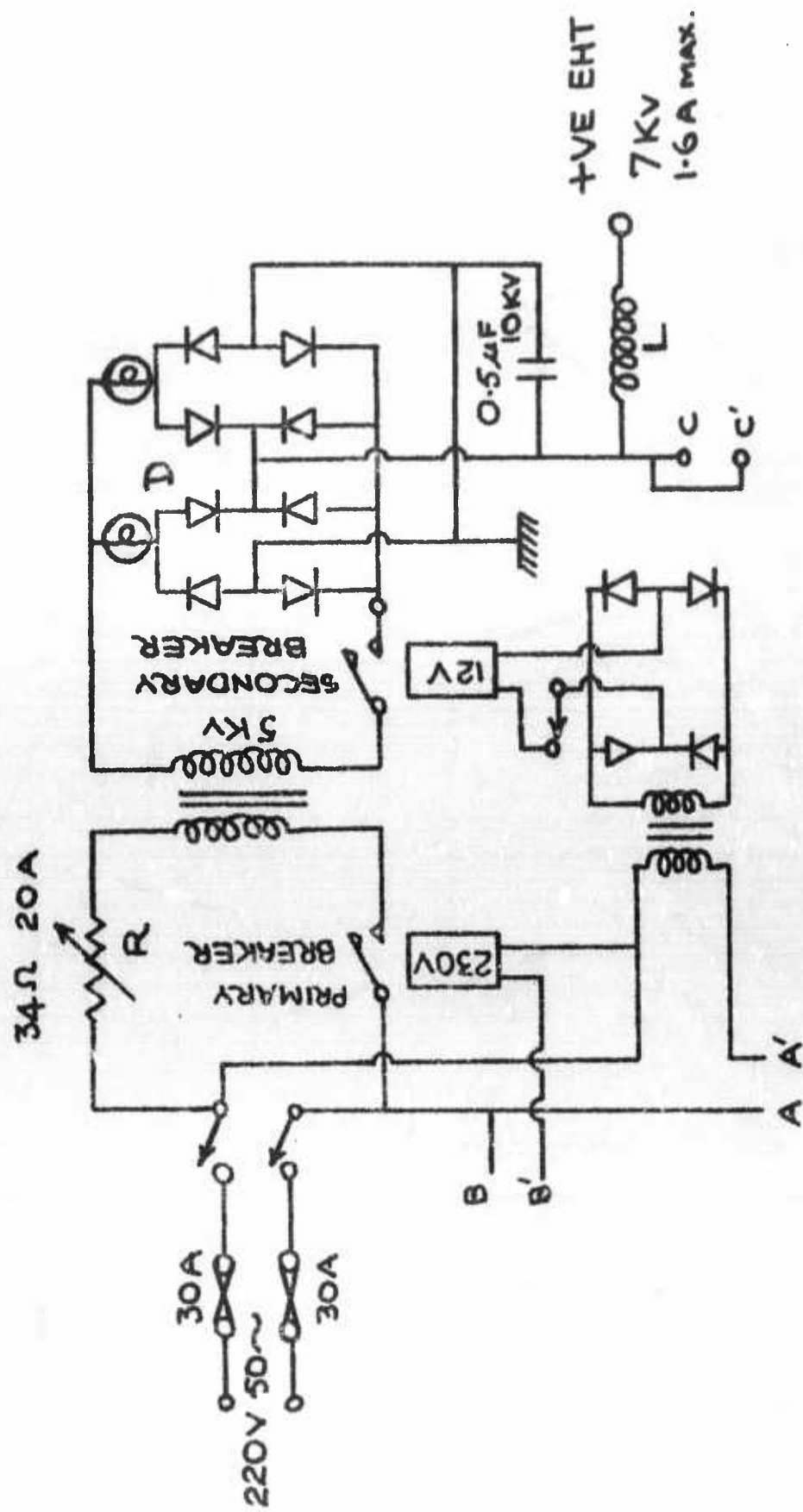


FIG. 6 E.H.T. CHARGING CIRCUIT.

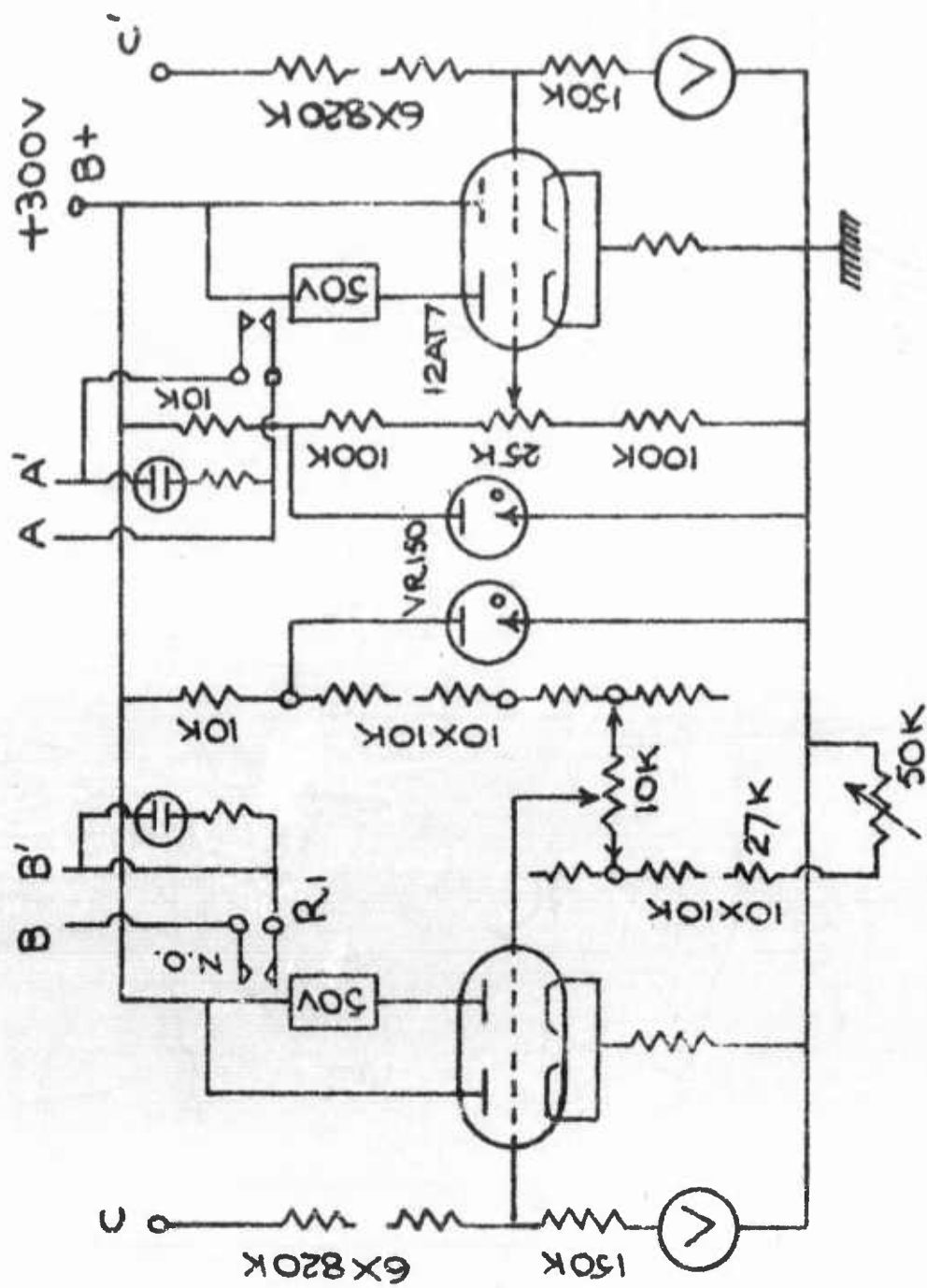


FIG. 7 CONTROL UNIT FOR CHARGING CIRCUIT.

are arranged as shown in Fig. 8 in the form of a delay line. The coils in this delay line are made from copper rod and designed so as to reduce the ohmic losses to negligible proportions. The delay line was designed to discharge through the two flash-tubes in series giving an approximately rectangular pulse with a width of about one millisecond. In this discharge the maximum power transferred is about 9000 joules. The actual observed shape of the pulse is described below.

#### The Laser Head

The laser head is a commercially produced unit with a double elliptical cavity, containing two E.G. & G., FX 66 flash tubes and a 16 x 1 cm. ruby rod. The flash tubes and the ruby are both water cooled using separate pumping systems with capacities of about five litres per minute and ten litres per minute respectively. At the present time the maximum discharge rate of 10 per minute has not yet been tested but the system has been found to work perfectly at rates of up to 2 per minute. As explained earlier, the wavelength of the laser changes with temperature and it has been found necessary to reduce the temperature of the water cooling the ruby to about 20°C. The flash tubes are triggered from windings round the flash-tube water jackets. These are energised by pulse transformers giving output voltages of about 50 kilovolts. The timing of the trigger pulse is described later.

Measurements have been made on the current pulse through the flash-tubes to see how well this fitted the original design parameters. The pulse was measured by recording the voltage across a very low resistance placed in series with the flash-tubes. The current pulse

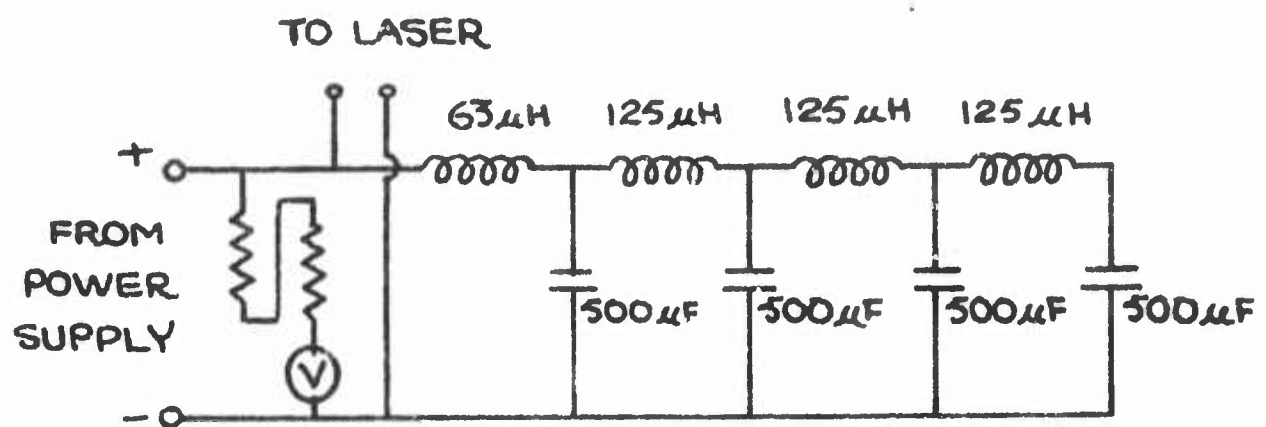


FIG. 8 ENERGY STORAGE AND PULSE FORMING NETWORK.

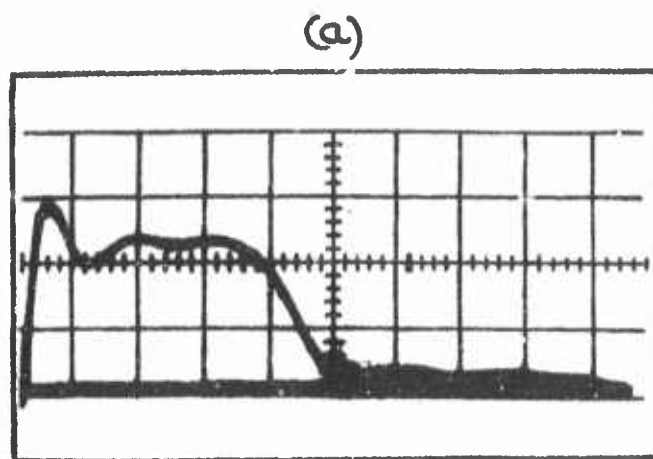
for an input of 5000 joules is shown in Fig.9(a). It can be seen that the maximum current is about 2000 amps and the pulse duration is about 2 milliseconds, rather longer than the design figure. It is believed that this difference is probably due to the fact that in designing the delay line no allowance was made for the possible inductance of the capacities. As yet, no effort has been made to alter this; the effect on the output power of the laser appears to be small and the lower current has the effect of increasing the flash-tube life.

The laser Q-spoiler is of the rotating prism type, the laser firing only when the prism is in an exactly symmetrical position with respect to the ruby rod. The rotation rate of the Q-spoiler may be varied between about 20,000 and 24,000 per minute and a pulse is generated once each revolution, about two milliseconds before the firing position. This, when suitably delayed, is used to trigger the flash-tubes. The delay between this trigger and the time of firing of the laser is variable and measurements have been made on -

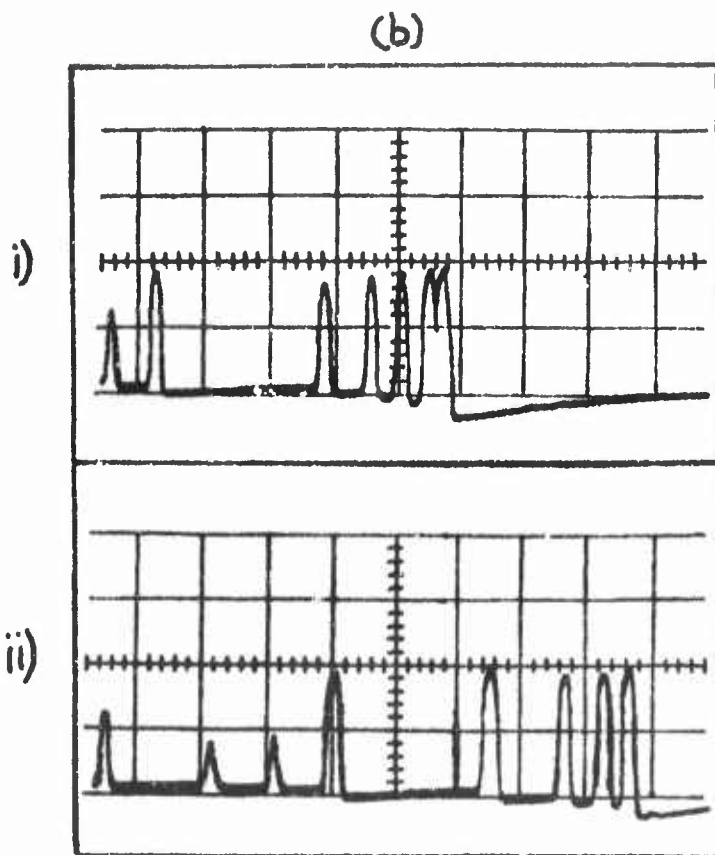
- a) the pulse shape of the laser output at 6943 Å, and
- b) the output power as a function of flash-tube input power and the delay time between triggering and firing.

Fig. 9(b) shows measurements made on the laser output waveform for two different input energies. In both cases the output consists of several pulses contained in rather less than 10  $\mu$ -seconds. The reason for the multiple pulsing is not clear but, as the total duration is well within that permissible for the experiment no efforts have been made yet either to study or to alter this.





SCALE  
 VERTICAL:  
 $800 \text{ AMP. CM}^{-1}$   
 HORIZONTAL:  
 $500 \mu \text{ SEC. CM}^{-1}$



SCALE  
 $1 \mu \text{ SEC. CM}^{-1}$

$1 \mu \text{ SEC. CM}^{-1}$

FIG. 9 (a) FLASH TUBE CURRENT WAVEFORM.

(b) LASER OUTPUT WAVEFORMS.

i) 5000 JOULES INPUT.

ii) 8000 JOULES INPUT.



The output energy has been measured calorimetrically, using two forms of detector - (i) an oxidised disc of copper foil with a thermocouple soldered to the centre and (ii) a cone of copper foil, oxidised on the inside, with a thermocouple attached near the apex of the cone. These measurements are very simple and are not likely to be very accurate but they do enable an estimate to be made of the power in each pulse. It is also possible to study how this varies with the timing of the Q-spoiler in relation to the triggering of the flash-tubes. The results of these measurements are shown in Fig.10 where it can be seen that the laser output is 4-6 joules and reaches its peak with a delay of about 1.5 milliseconds.

#### Special Problems connected with the Laser Output

Two special problems arise in connection with the signal from the laser. These were outlined in Section 2.3 and are connected with (i) the fluorescence of the ruby and (ii) the change of wavelength of the laser with temperature.

(i) As explained earlier the energy output at  $6943 \text{ \AA}$  from the ruby is not completely contained within the giant pulses already described. These are followed by the much weaker fluorescence at the same wavelength which persists for about two milliseconds. This, when scattered from the lower atmosphere, gives a signal of the same order of magnitude as the main pulse when scattered from the upper atmosphere. This represents an intolerable level of degradation of the signal to noise ratio and has necessitated the construction of a rotating shutter in front of the laser. This is shown schematically in Fig.11 and

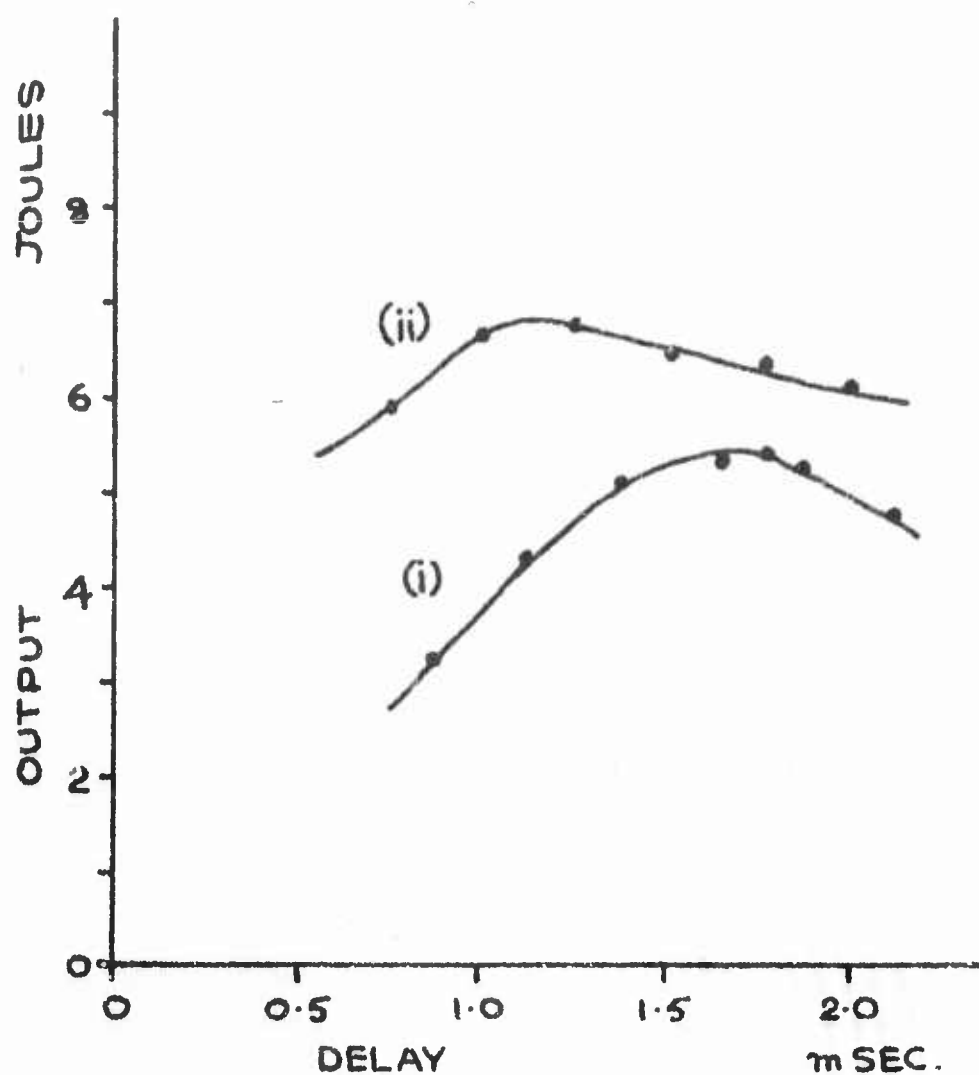


FIG. 10 VARIATION OF LASER OUTPUT WITH  
DELAY BETWEEN FLASH-TUBE  
TRIGGERING AND FIRING OF LASER.  
i) 5000 JOULES INPUT.  
ii) 8000 JOULES INPUT.

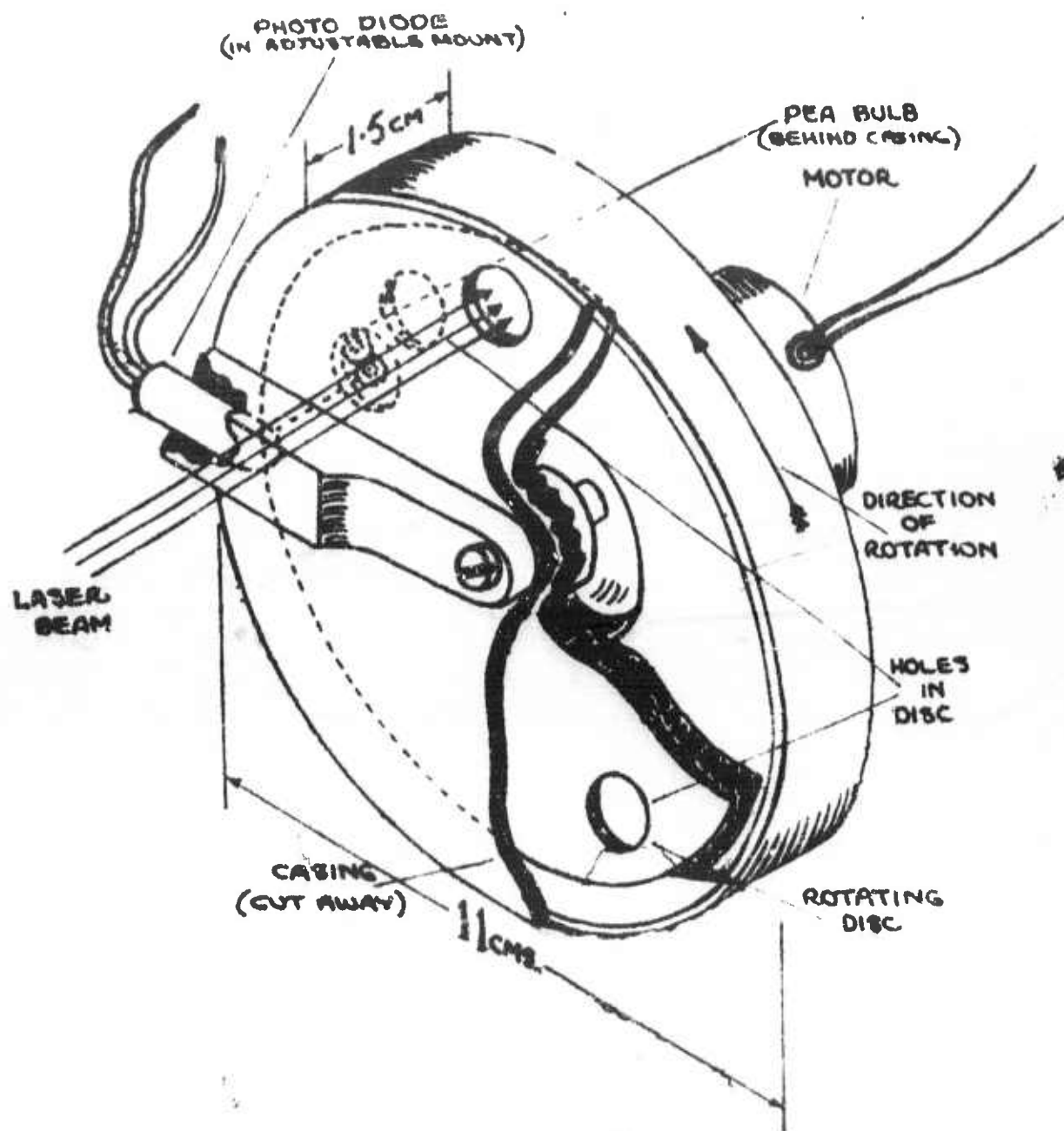


FIG. 11 HIGH-SPEED SHUTTER.

consists of an accurately balanced steel disc with two diametrically opposed half-inch holes. This is driven from an A.C. hysteresis motor at approximately the same speed as the Q-spoiler. The laser is arranged to be fired only when one of the holes is directly in front of the beam. The size of the hole and the rotation rate are such that the main beam is permitted to pass but the fluorescence is cut off about 100  $\mu$ -seconds after firing.

(ii) Also mentioned earlier is the use of water to cool the ruby. This is to prevent damage to the ruby due to heating from the flash. Even though this cooling water passes fairly rapidly it is still believed that the ruby suffers a significant rise in temperature. This would not be important were it not for the fact that, as explained in Section 2.3, the wavelength of the light emitted changes by about 1 Å for a 50°C rise in temperature. A small rise up to about 45°C is sufficient to carry it into the region of the water vapour absorption line at 6943 Å. The effect of this has been noticed as a very pronounced decrease in the intensity of scattering from the high atmosphere, presumably due to absorption lower down, after the laser has been running for a time. The actual amount appears to depend upon the atmospheric conditions but at times has been as much as 70%. It has been found that reducing the temperature of the water in the cooling system by about 10°C is sufficient to remove this effect and this is now the normal procedure.

#### The Control System

A block diagram of the operations sequence for firing the laser is shown in Fig.12. The requirements of this are that -

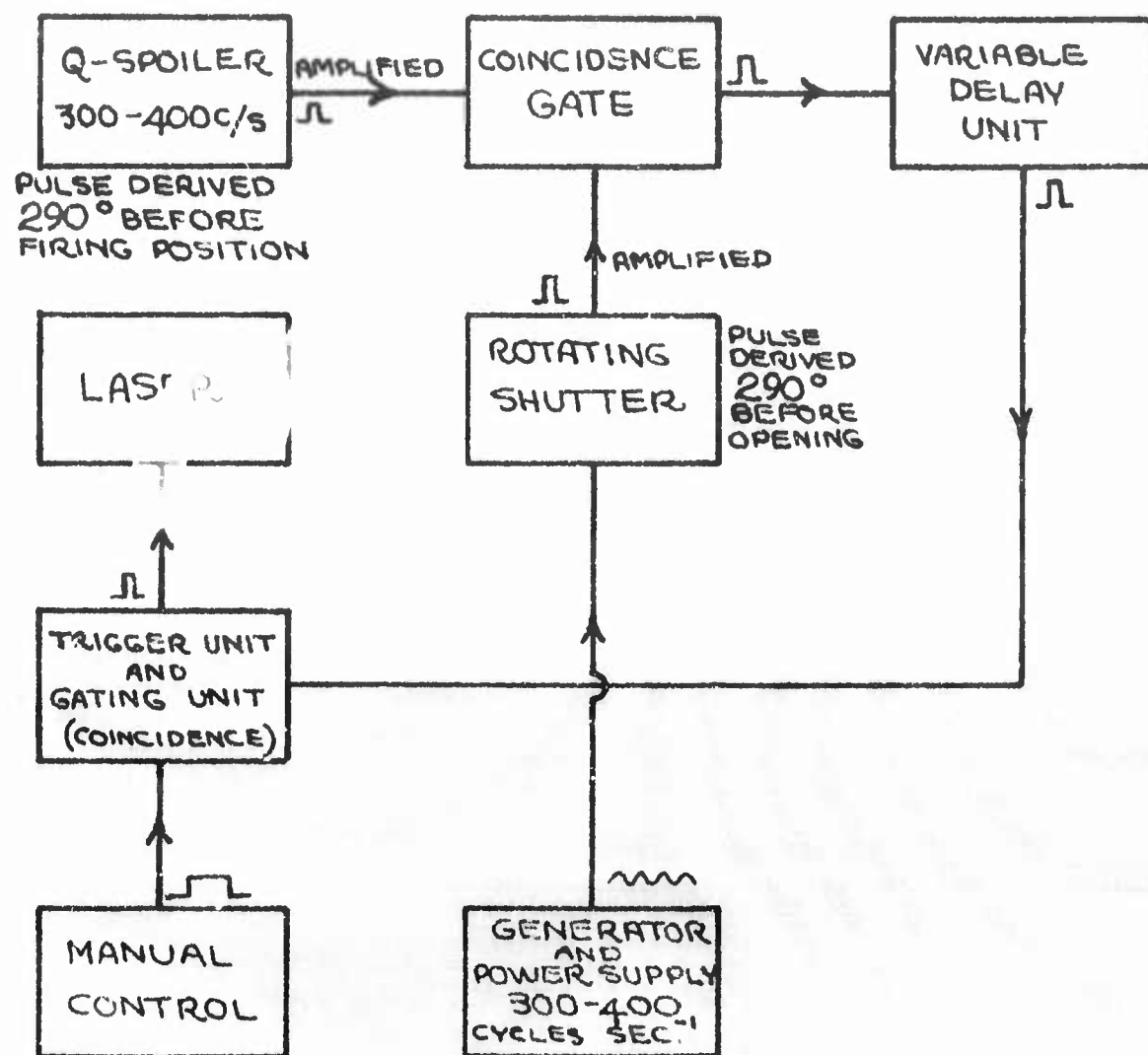


FIG.12 CONTROL SEQUENCE FOR TRANSMITTER.

- i) there is overall manual control,
- ii) the laser is only fired when the rotating shutter is in the correct position, and
- iii) the delay between the triggering of the flash-tubes and the firing of the laser may be set to a desired value.

A pulse is derived from the Q-spoiler once per revolution at approximately 0.808 of its period before the position for firing the laser. A similar pulse is derived from the rotating shutter at exactly the same fraction of its period before it opens. The rotation rate of these two units is set to differ by about one cycle per second and the pulses from them are amplified and passed into a coincidence gate; coincidence will therefore occur about once per second. The output pulse from the coincidence gate is passed into a variable delay and then into another gate which may be opened with a manual switch. The output pulse from this is used to trigger the flash-tubes. Using this arrangement any suitable delay may be included between the triggering of the flash-tubes and the firing of the laser. In addition the laser will only fire when the Q-spoiler and the shutter are in synchronism.

#### The Optical System

The beam from the laser is collimated, as shown in Fig.4 via a diverging lens, a dielectrically coated  $45^\circ$  mirror and a 23 cm. diameter parabolic mirror. The focal lengths of these are 7.6 cm. & 150 cm. respectively giving a reduction in angular beamwidth of approximately 20:1. The shape of the beam from the laser has been examined by the simple process of firing it at pieces of blackened photographic paper



placed at various distances from the laser, and observing the burn-marks. In this way it has been found that the beam is approximately circular in shape and has a total angular beamwidth of about half a degree (nine milliradians). When used in conjunction with the collimator this is reduced to about 1.5 minutes of arc (0.4 milliradian).

The 20 cm. parabolic mirror is supported on one fixed point and two adjustable micrometers. Using these the collimation of the receiving and transmitting beams may, as will be explained in Section 3.4, be carried out to an accuracy of up to 0.1 minute arc.

### 3.3 The Receiver

A block diagram of the receiver is shown in Fig.13.

#### The Receiving Mirror and Apertures

The main receiving mirror is 50 centimetres in diameter, it has a focal length of 250 centimetres and is ground to astronomical accuracy. It is rigidly mounted onto a flat glass plate set into the floor of the laboratory. The mirror is chemically silvered, the coating deposited being replaced at intervals of about four months. The beam from the mirror is focussed via a  $45^\circ$  mirror onto an aperture which may be varied from 0.5 mm to approximately 10 mm. in diameter. Table 3. shows the angular beamwidths corresponding to different sizes of the aperture.

ATMOSPHERIC  
SCATTERING

----- OPTICAL LINK

——— ELECTRICAL LINK

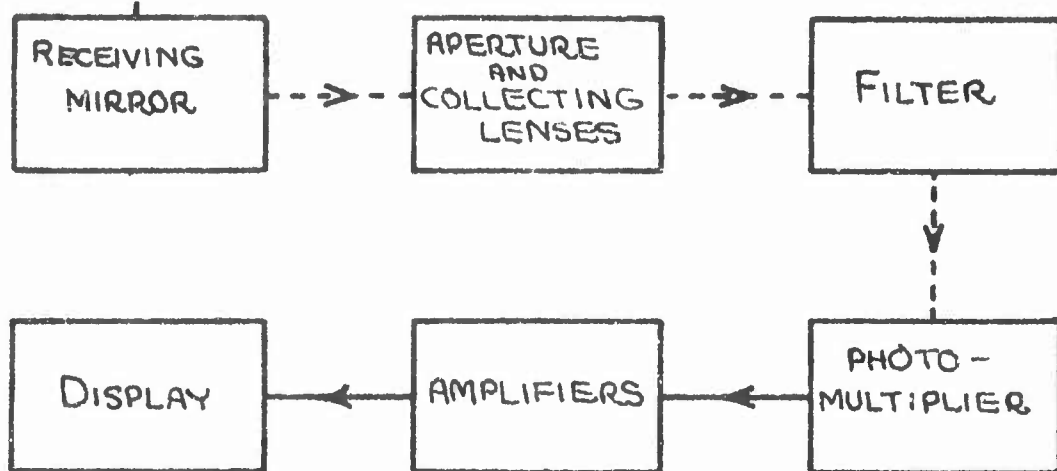


FIG.13 BLOCK DIAGRAM OF THE RECEIVER.

TABLE 3

Aperture sizes and corresponding beamwidths

Aperture diameter	Total angular beamwidth
10.0 mm.	14 minutes arc (4 millirad.)
5.0 mm.	7 " (2 " )
2.5 mm.	4 " (1 " )
1.0 mm.	1.4 " (0.4 " )
0.5 mm.	0.7 " (0.2 " )

(not all available sizes are shown above)

The smallest aperture size completely containing the transmitted beam will be 1.0 mm. When this aperture size is used a calculation based on the geometry shown in Fig.14 shows that the beams commence to overlap at a height of 0.3 km. and that the overlap is 90% complete at a height of about 8 km.

The filters

Behind the aperture there is a converging lens which renders the beam parallel again. This has a focal length of two inches and produces a beam of diameter rather less than half an inch. Provision is made for the insertion into this beam of narrow-band filters centred on or near  $6943 \overset{\circ}{\text{\AA}}$ . Two filters are used, one with a width of  $20 \overset{\circ}{\text{\AA}}$ , for night-time studies, is inserted straight into the beam. The other has a width of  $4 \overset{\circ}{\text{\AA}}$  and is centred on  $6945 \overset{\circ}{\text{\AA}}$ . This is mounted in a special rotatable housing so that its centre frequency may be set to exactly  $6943 \overset{\circ}{\text{\AA}}$ . This filter is not used at night-time

OVERLAP 90% COMPLETE AT 8 Km

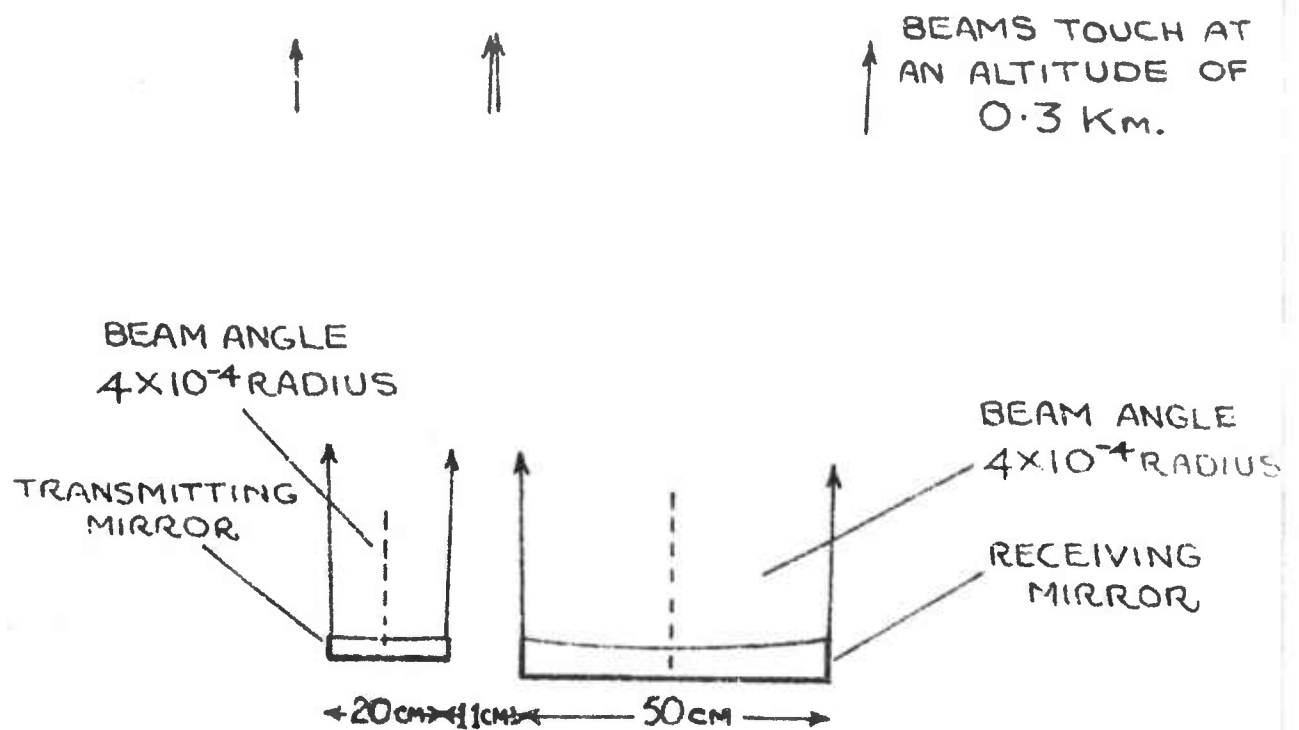


FIG. 14 THE PHYSICAL ARRANGEMENT OF THE TRANSMITTED AND RECEIVED BEAMS.

as it has a rather lower transmission factor than the other (4% against 60%). It is used during the day when it is necessary to reduce the sky background noise to as low a value as possible.

As well as the narrow-band filters, which have to be inserted into the beam after it has been collimated, there is provision to insert neutral and polarising filters into the converging beam. Neutral filters ranging from 50% to 0.5% are available and these may be used in combination if necessary. The introduction of these and the polarizing filters into the converging rather than the parallel beam does not materially affect the performance of the system.

#### The Photomultiplier, Amplifiers and Display

The photomultiplier tube used is an E.M.I. type 9558A. This is designed for astronomical use and combines a enhanced red response with low noise current. In spite of this the quantum efficiency at  $6943 \text{ \AA}$  is only about 3%. The photomultiplier is housed inside a light-tight and air-tight housing sealed onto the mounting containing the narrow-band filter and the collimating lens and aperture. As explained in Section 3.1, the whole of this assembly is mounted on an optical bench fixed to a steel beam. The output from the photomultiplier is fed directly into a pulse pre-amplifier placed inside the same housing. The signal is then fed into another wide-band amplifier and the output from this taken to a Tektronix oscilloscope. It is intended later to count this output in range-gated intervals and to store in core storage. For the moment however, the signal is displayed on the oscilloscope and photographed with a polaroid camera. In order to be

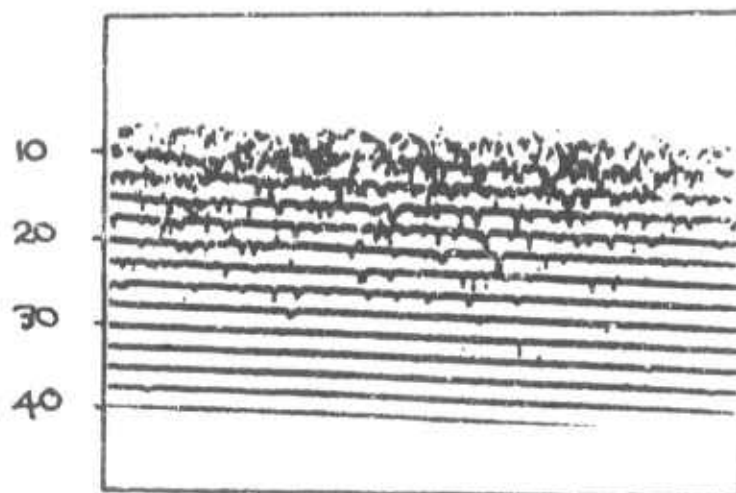
able to show as much information as possible, the display chosen is in the form of a raster. A differential Y-amplifier is used in the oscilloscope, the signal being fed into one input and a ramp waveform into the other. The time-base chosen for the X-deflection has a sweep period of 10  $\mu$ -seconds and a dead-time of 5  $\mu$ -seconds. When investigating the higher regions of the mesosphere, from which the scattered photons are well spaced, about 30 lines can be displayed across the face of the tube, this corresponds to a height range of about 50 kilometres. A typical display taken under these conditions is shown in Fig.15(b). When looking at the lower atmosphere, where echoes are more frequent, it is necessary to display fewer lines to avoid confusion. Such a display is shown in Fig.15(a).

In the display shown in Fig.15(b) the pulses from the photomultiplier appear quite distinct and may be individually counted without effort. Sometimes, when a pulse is weak, it is difficult to distinguish it from noise but, provided a constant criterion is employed, this does not lead to serious error. In Fig.15(a) the problem is not so easy, on the upper lines the pulses are overlapping and it is found that when more than about forty per line occur the counting technique is unreliable. In this case a neutral filter is inserted into the beam, reducing the count to a readable value. This procedure does of course raise the random error, which is simply proportional to the square root of the total count. Averaging over several shots however is sufficient to reduce this to tolerable proportions.



HEIGHT IN KILOMETRES

(a)



HEIGHT IN KILOMETRES

(b)

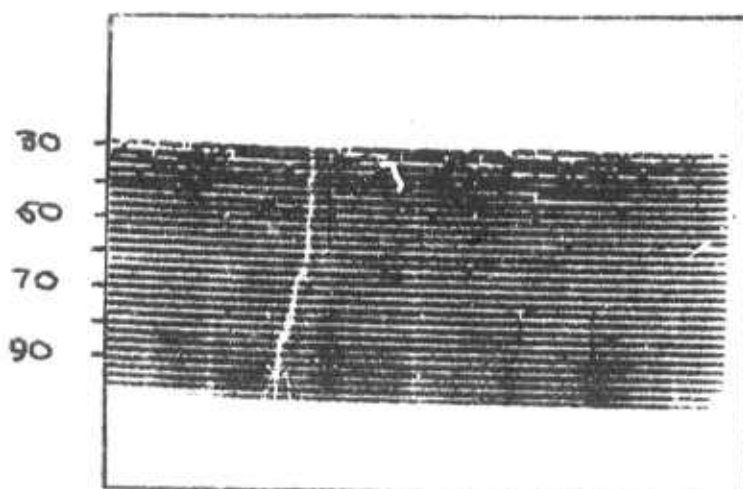


FIG. 15 THE FORM OF THE DISPLAY USED  
FOR RECORDING AND COUNTING ECHOES

(a)  $5-41\frac{1}{2}$  km

(b)  $30-101\frac{1}{2}$  km

### The Control System for the Display

The control system for the display is shown as a block diagram in Fig.16. The purpose of this is to be able to vary the height range displayed and also to know accurately what this range is.

A pulse is derived from a photo-diode placed in the path of the outgoing laser beam. This pulse is used to trigger a ramp waveform which is used as one of the inputs to the Y-amplifier in the display. As it is not possible to study the echoes received from the whole height-range from ground level upwards, the ramp waveform is also used to generate a delayed pulse. This pulse is then used to gate the free-running time-base of the oscilloscope so that a pre-determined height-range may be displayed. Also shown in Fig.16 is the circuit used to calibrate the delays employed. A digital timer is used and pulses are derived coincident with the laser pulse, the beginning of the display and the end of the display. By timing the intervals between these, using the digital timer, an accurate calibration may be made of the setting of the displayed height-range.

### The Signal-to-noise Ratio

The fundamental problem in the detection of a very weak scattered echo is, as explained in Section 2.3 to discriminate against noise. This noise may arise either from the photomultiplier itself, the faint glow from the night sky or the fluorescence of the laser described before. When observing echoes it is quite possible in a run to take up to one hundred shots. Some integration over a narrow height range is usual but this is never more than ten kilometres.

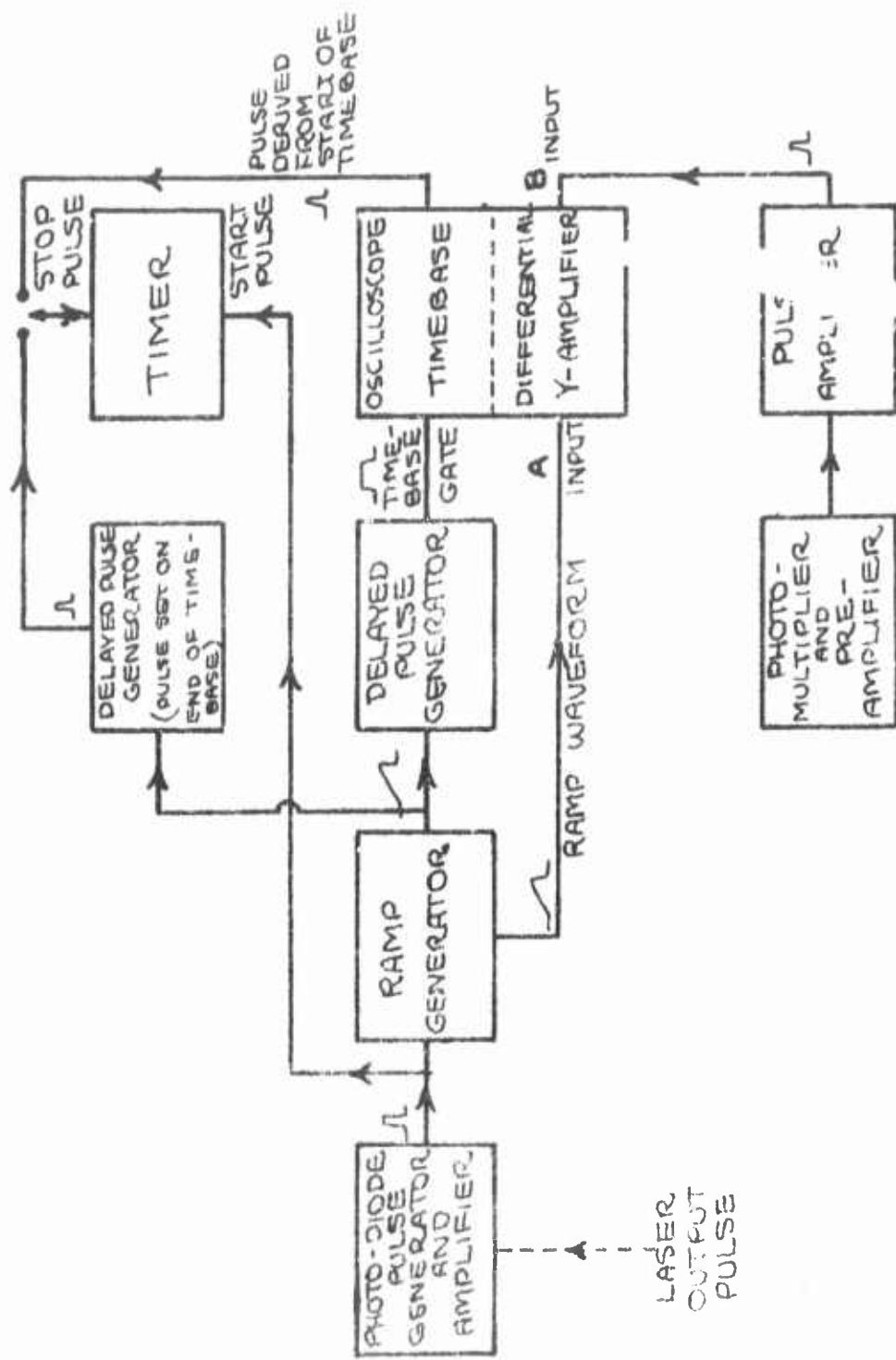


FIG. 16 CONTROL SYSTEM FOR THE DISPLAY.

With the display as described above and a series of 100 shots this would amount to a total integration time of 4000  $\mu$ -seconds. In order to make full use of the signal recorded during this time it is desirable to reduce the background noise to negligible proportions, this means to one count or less. In other words the background count should not be more than 250 pulses per second. Table 4 shows the actual contributions from the three main noise sources.

TABLE 4.

Background noise measurements

<u>Source</u>		<u>Counts per second</u>
Photomultiplier		
At room temperature		14,000
Cooled with ice		3,000
Cooled with cold nitrogen		50
Sky-noise		
Night-time	0.10 cm. aperture	about 10
Day-time	0.10 cm. aperture and 4 A filter	$2 \times 10^6$
Fluorescence	0.10 cm. aperture	$10^5$
Received signal		
From 50 km.		$4 \times 10^4$
From 70 km.		4,000

It can be seen that at night the fluorescence of the laser is by far the most serious of the three sources. This necessitated the construction of the rotating shutter already described. The other large contribution is from the photomultiplier. At room temperature this is about 14,000 per second and it is reduced to this value only when thoroughly desiccated in an atmosphere of dry nitrogen. It can be seen from the table that cooling the tube has a very marked effect and this is without any appreciable reduction in sensitivity. The cooling technique which is now used is to drive the nitrogen in the photomultiplier housing through a U-tube immersed in liquid air. This is done by means of a scaled pump and the gas from the U-tube passes through a short connecting length of tubing and impinges straight onto the face of the photomultiplier. The exact temperature drop is uncertain but the noise counting rate is reduced to the negligible value of about 50 per second. It was mentioned earlier that the  $20 \text{ \AA}$  wide filter is placed in the same housing as the photomultiplier tube. To avoid cooling this, with consequent change in pass-band and to prevent condensation, a heating coil is used to maintain this end of the housing at room temperature. It was also mentioned that other sources of noise appear to be present and that these are at present under investigation. The rate of these is between 1000 and 2000 per second. This, while fairly low can be a nuisance when receiving signals from above 7000. It may be noted here that it is important to prevent direct electrical interference from travelling from the transmitter to the receiver. The current oscillations in the flash-tubes are of

the order of several thousand amps and careful filtering is necessary to prevent transients from passing into the electric mains and out again into the receiver amplifiers.

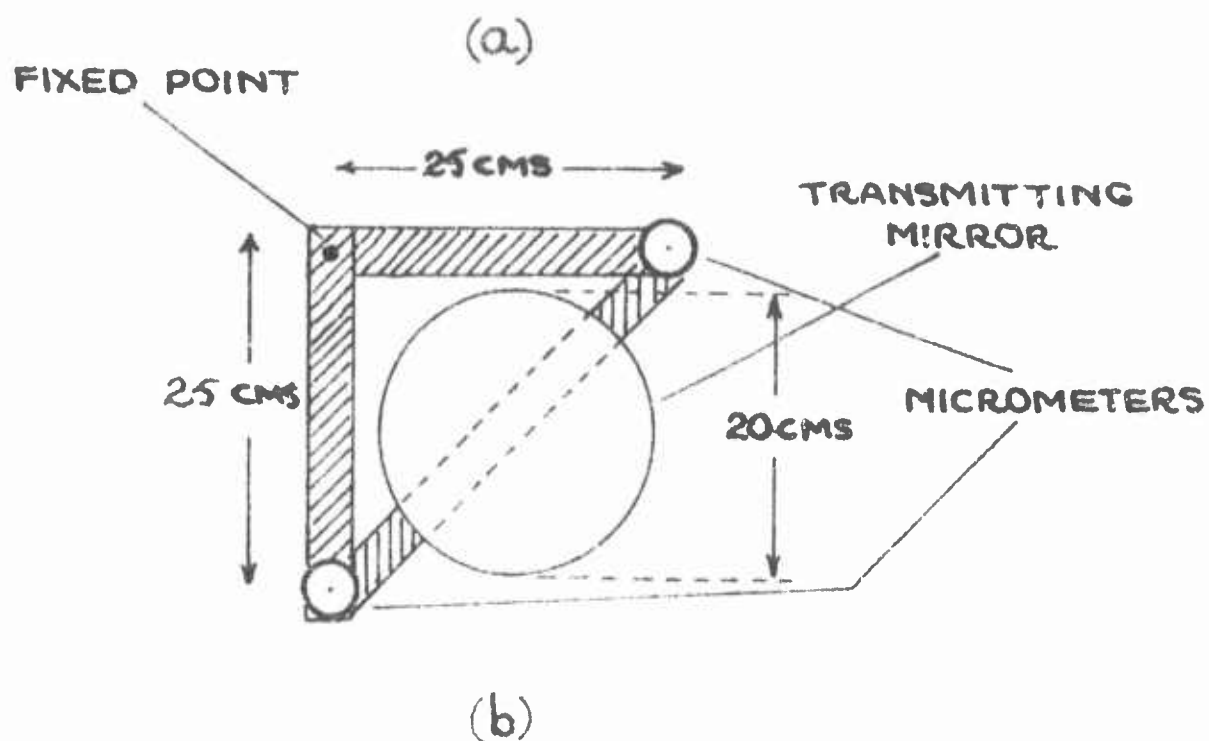
During the day the background sky noise is very high and the other effects discussed above may be neglected. To reduce this sky background to a minimum value, the narrow  $4 \text{ \AA}$ -wide filter is used and the smallest permissible aperture. Under these conditions as explained before, it is possible to detect echoes up to 30 kilometres.

#### 3.4. The Alignment of the Receiver and Transmitter

The widths of the transmitting and receiving beam are, as explained in Sections 3.2 and 3.3, only about 1.5 minutes of arc across. The alignment of these is necessarily a fairly difficult procedure. The alignment is carried out using the micrometer adjustments beneath the transmitting mirror which are arranged, as shown in Fig. 17 (a) at the ends of two 25 cms. arms. A setting accuracy of 0.0005 cm. is possible with these micrometers, corresponding to an angular shift of 0.1 minute arc.

The procedure adopted is to first of all adjust both the receiving and transmitting mirrors so that the axes are approximately vertical. This may be done, using plane mirrors and a bowl of mercury as a horizontal reflecting surface, to an accuracy of perhaps  $0.1^\circ$ . This means that, if the receiving aperture is opened to its widest extent (as shown in Table 3.), the resultant wide receiving beam will now encompass the narrow transmitting beam.

Having reached this stage, the process of collimating the beams



SETTING OF MICROMETER A (IN UNITS OF  $\cdot 025$  MM)

	87	88	89	90	91	92	93
96				30			
97				61			
98	33		52	66	58		39
99				70			
100				68			
101				58			
102				33			

SETTING OF MICROMETER B

THE NUMBER OF PHOTONS RECEIVED FROM ABOVE 15 Kms (USING A 10% FILTER) IS SHOWN IN THE SQUARE APPROPRIATE TO THE MICROMETER SETTING.

FINAL SETTING CHOSE

A. 90

B 99

FIG 17(a) THE MOUNTING OF THE TRANSMITTING MIRROR.

(b) PHOTON COUNTS FOR VARIOUS MICRO-METER BETTINGS FOR A 1.0MM RECEIVING APERTURE.



is one of successive approximation. The receiving aperture is opened wide and the laser is fired. A note is made of the echo count received from a given height. The receiving aperture is then reduced and the process repeated until the observed count begins to drop. This implies that the receiving beam no longer overlaps the transmitting beam. The micrometers beneath the transmitting mirror are then adjusted in suitable steps and the echo amplitude determined for a number of settings of the micrometers covering a range such as shown in Fig.17(b). The settings of the micrometers which give the maximum count are noted and they are adjusted to these values. The receiving aperture diameter is then halved and the process repeated with smaller micrometer steps. This is successively repeated until the smallest aperture (1.00 mm.) is reached. This process as described sounds tedious and lengthy, but, with practice, may be carried out very quickly. Owing to the settling of various parts of the apparatus it has been found desirable to check the alignment of the beams at intervals of every few weeks.

#### 4. THE EXPERIMENTAL RESULTS

##### 4.1 Introduction

Most of the year has been occupied with the construction and testing of the equipment already described and no continuous period of experimental observation has been attempted. Observations have of course been made at various altitudes in the process of proving the equipment and the results of these are described in this section. Such runs as have been done are short in length and should not be taken as indicative of the final performance of the instrument.

As explained in Section 2.1 the product  $Ch^2$ , where  $C$  is the observed photon count and  $h$  the height, is proportional to the scattering cross-section of the atmosphere at the height  $h$ . Observations have been made on  $C$  over heights extending from 10 to 90 km. using a series of neutral filters and the simple counting technique explained earlier. Values of  $C$  and  $Ch^2$  for a series of 105 shots made during one single week are given in Table 5 and  $Ch^2$  is shown graphically in Fig.18. Also shown in Fig.18 are the values of  $np_R$  taken from Table I and normalized to fit the experimental points at an altitude of 30 kilometres. It can be seen that the experimental results above 70 km. are subject to a high random error. This is particularly true in these results as they were taken before the introduction of the rotating shutter to eliminate the effect of fluorescence. However the general variation of  $Ch^2$  agrees well with the theoretical curve and a more detailed comparison is made below. Also clearly visible in the graph

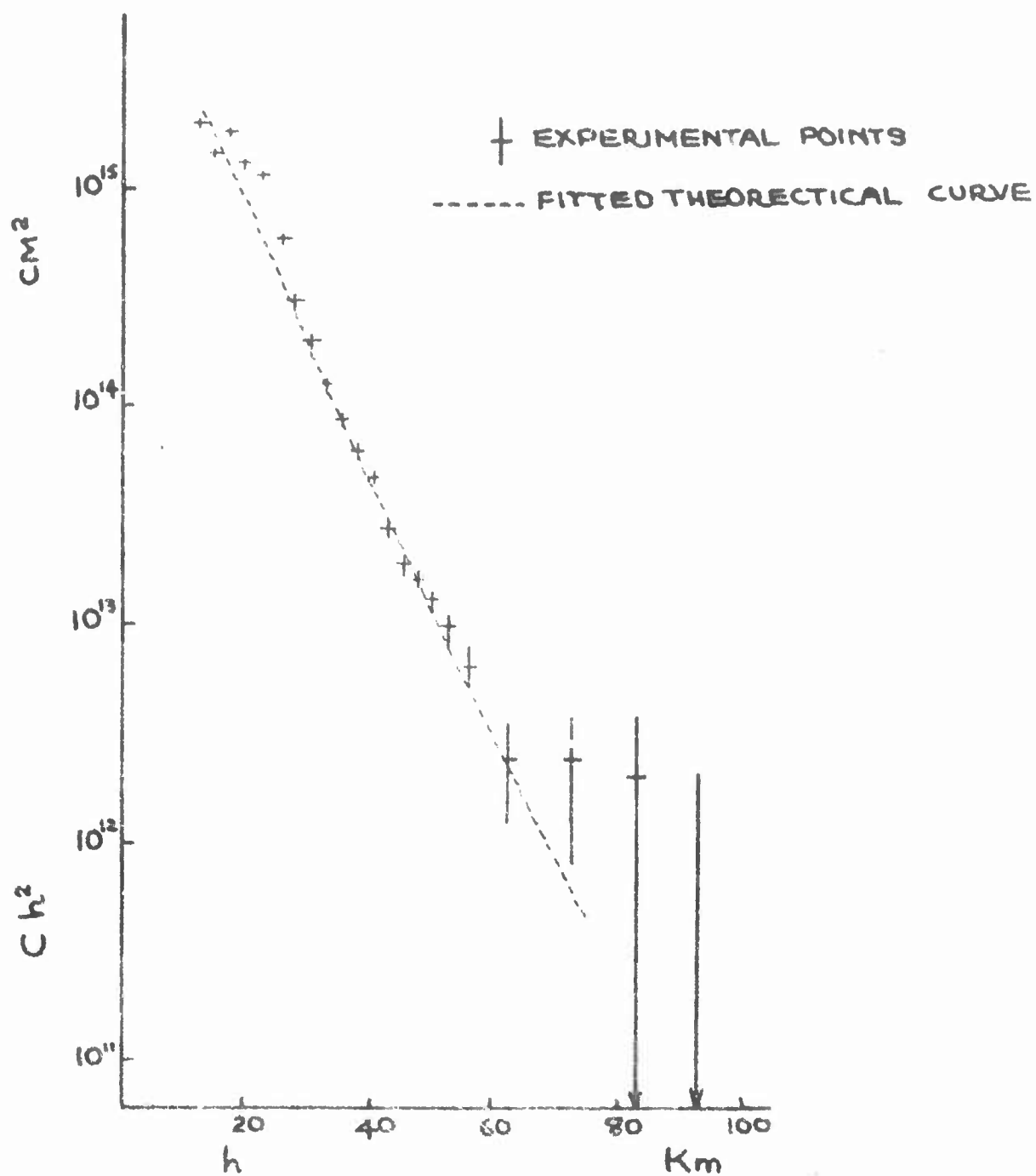


FIG. 18 EXPERIMENTAL VARIATIONS OF  $Ch^2$  WITH ALTITUDE. (C IS THE COUNT IN A  $1\frac{1}{2}$  Km INTERVAL).



TABLE 5

Measurements on the Scattered Signal Intensity fromDifferent Altitudes

Height h km.	Photon Count C		$C h^2$ cm <sup>2</sup>
13	1150 ± 45	( 1.94 ± 0.07 )	$\times 10^{15}$
15½	604 ± 30	( 1.45 ± 0.07 )	$\times 10^{15}$
18	560 ± 30	( 1.83 ± 0.09 )	$\times 10^{15}$
20½	310 ± 13	( 1.30 ± 0.05 )	$\times 10^{15}$
23	219 ± 10	( 1.16 ± 0.05 )	$\times 10^{15}$
25½	91 ± 5	( 5.9 ± 0.3 )	$\times 10^{14}$
28	38.3 ± 1.8	( 3.0 ± 0.15 )	$\times 10^{14}$
30½	21.4 ± 0.4	( 1.99 ± 0.04 )	$\times 10^{14}$
33	11.4 ± 0.3	( 1.24 ± 0.03 )	$\times 10^{14}$
35½	6.66 ± 0.3	( 8.39 ± 0.3 )	$\times 10^{13}$
38	4.28 ± 0.2	( 6.18 ± 0.3 )	$\times 10^{13}$
40½	2.81 ± 0.2	( 4.61 ± 0.3 )	$\times 10^{13}$
43	1.47 ± 0.12	( 2.72 ± 0.2 )	$\times 10^{13}$
45½	0.91 ± 0.12	( 1.88 ± 0.2 )	$\times 10^{13}$
48	0.70 ± 0.09	( 1.61 ± 0.2 )	$\times 10^{13}$
50½	0.47 ± 0.08	( 1.20 ± 0.2 )	$\times 10^{13}$
53	0.33 ± 0.07	( 9.3 ± 2.0 )	$\times 10^{12}$
56½	0.20 ± 0.05	( 6.4 ± 1.6 )	$\times 10^{12}$
63	0.06 ± 0.03	( 2.4 ± 1.2 )	$\times 10^{12}$
73	0.045 ± 0.03	( 2.4 ± 1.6 )	$\times 10^{12}$
83	0.03 ± 0.03	( 2.0 ± 2.0 )	$\times 10^{12}$
93	-0.005 ± 0.03	( -4.0 ± 25 )	$\times 10^{11}$

(Counts given above are for a ten  $\mu$ -second or 1½ km. interval).

is the enhancement in the scattering profile near twenty kilometres due to the aerosol layer at this height.

#### 4.2 Comparison with Rayleigh Scattering Theory

The experimental points in Fig.18 are sufficiently good to enable estimates to be made of the scale height and hence of the temperature in the region 30-60 kilometres. From the slope of a line drawn through these points it may be deduced that the scale height at 35 kms. is 6.1 kilometres and rises to about 7.6 kilometres at a height of 45 kilometres. This corresponds to a temperature change of from  $208^{\circ}\text{A}$  to  $260^{\circ}\text{A}$ . This agrees very well with the values for the standard atmosphere (Cole and Kantor, 1963).

It is also of interest to compare the values for the scattered photon count in Table 5 with the predicted values given in Table I. Before this can be done some estimate must be made of the losses of the transmitting and receiving systems. A brief list of the estimated losses is shown in Table 6. from which it can be seen that the efficiency of the complete system (including the photomultiplier) was about 18%. This is a surprisingly low value, due chiefly to loss in the filter and to water vapour absorption. These measurements were made before the temperature of the ruby cooling water was controlled and it is estimated, on the basis of more recent measurements, that about 40% of the signal was absorbed by water vapour. Taking a representative level of 30 kilometres from Table I it then appears that a count of about 110 pulses would have been expected. In practice only 25 were obtained, a discrepancy by a factor of four. This is a serious factor

TABLE 6

Losses in the System for the Measurements shown in Table 5

<u>Component</u>	<u>Transmission or Reflection Efficiency</u>	<u>Remarks</u>
Transmitter		
Right angle Mirror	95 %	Including aperture limiting losses.
Concave Mirror	90 %	
Receiver		
Concave Mirror	85 %	Including obstruction losses
Right angle Mirror	90 %	
Convex lens	92 %	
20 Å filter	60 %	
Perspex Window	92 %	
Aperture	90 %	
Water vapour absorption	60 %	This is apart from the normal attenuation due to aerosol and molecular scatter- ing which has already been taken into account.
TOTAL	18 %	

which, if it could be eliminated, would enable the sensitivity of the equipment to be considerably increased. At the moment we are in ignorance as to its origin: it is possible that the estimate for absorption in the atmosphere is much too low, although it is difficult to believe that this could contribute a factor of four. This problem will be examined during the coming year and, it is hoped, a solution

found.

As remarked earlier, our equipment is considerably more sensitive than that believed to be in use by other workers. It is interesting to compare the amplitude of our scattered echo with that of Fiocco and his co-workers. In his paper in conjunction with Smullins in 1963, Fiocco obtained, over the same height interval, at a height of 40 kilometres, about one recorded photon for each twenty-five transmitted pulses. The value given in Table 5 is 2.8 for a single transmitted pulse and, as explained, this is about 40 % low. This indicates a value of about one hundred for the ratio of the sensitivities of the equipments.

#### 4.3 The Dust Layers

##### The lower dust layer

In Section 4.1 mention was made of the dust layer clearly visible between 15 and 30 kilometres. This has been observed on several occasions, during the day as well as the night. The data in Fig. 18 is shown redrawn to a larger scale in Fig. 19(a) and here the bifurcation of the layer can be seen very clearly. The actual enhancement of the signal over the expected Rayleigh scattering is by a factor of about two. These results agree well with those of both Elterman and Campbell (1964) and Fiocco and Grams (1964). It is perhaps a little odd that while the numerical value of the enhancement agrees better with Fiocco and Grams, the bifurcation, with the lower peak at or near the tropopause, is shown only by Elterman and Campbell. The possibility of this being a latitude variation must be borne in mind however.

In Section 2.2. the depolarisation of the scattered signal was



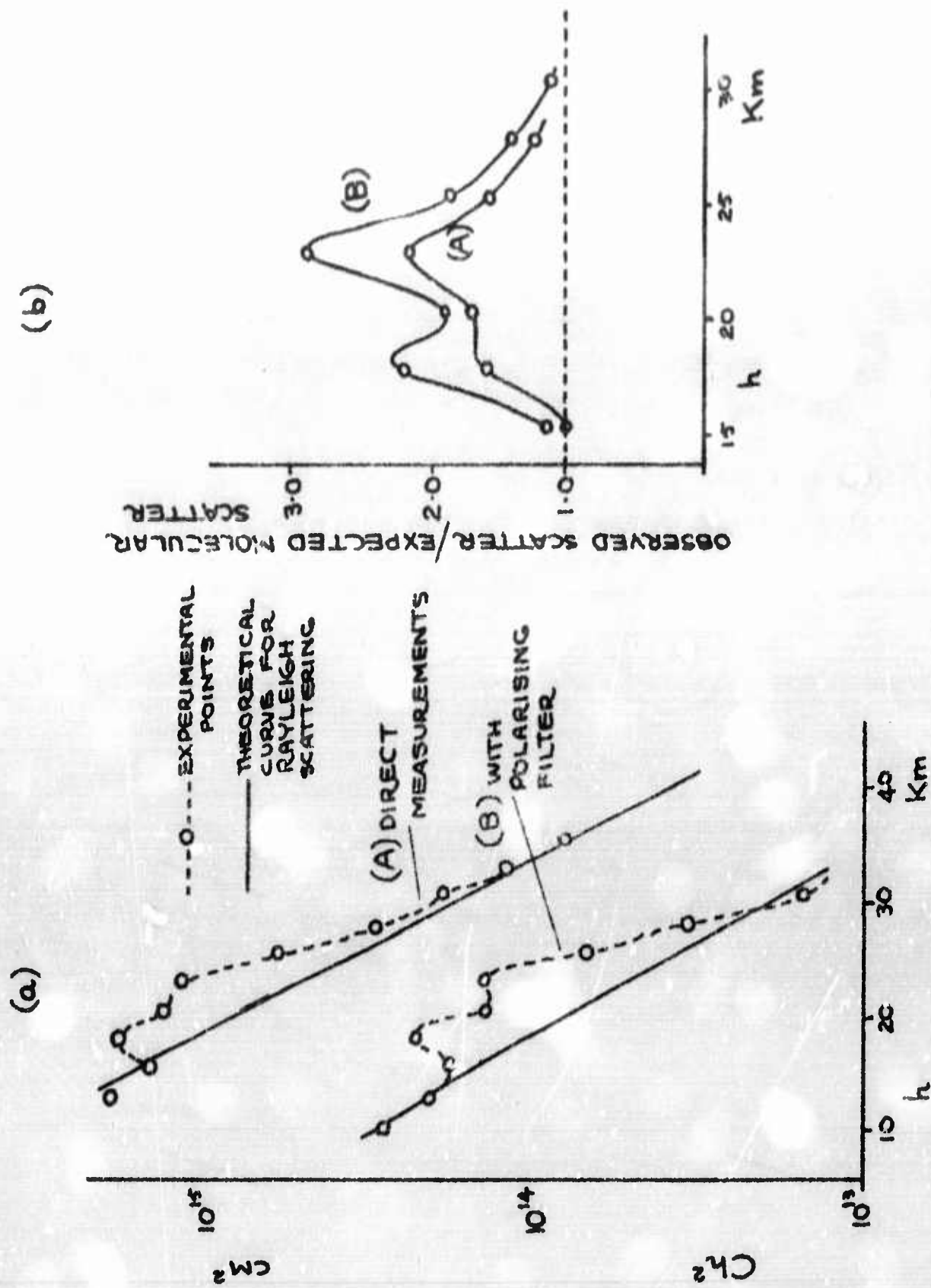


FIG. 19 SCATTERING PROFILES NEAR THE 20 KILOMETRE DUST LAYER, OBSERVED WITH AND WITHOUT POLARISING FILTERS.

discussed above. A series of observations have been made using a polarising filter in the receiving beam orientated to reduce the signal to a minimum. The results of this are also shown in Fig. 19(a). It can be seen that the molecular scatter is reduced by a factor of about twelve while that for the aerosol layer is reduced by a factor of only eight. This point is further emphasised in Fig. 19(b) where the ratio of total scatter to expected molecular scatter is plotted. It may be noted that below fifteen kilometres the signal is rather less than expected; this is partly due to reading errors and partly to the incomplete overlap of the transmitted and received beams. The maximum depolarisation values deducible from this data are 8% for the molecular scatter and 12% for the aerosol layer. The former, in particular, of these two figures should not be taken as an exact measure as it is doubtful that the polarising filter was set to an accuracy of better than  $5^\circ$ . The difference between the two is however significant and is of the order of that expected on theoretical grounds (Section 2.2.).

#### The Upper Dust Layers

In their paper of 1963 Fiocco and Smullin report dust layers existing at altitudes between 60 and 90 kilometres and between 110 and 140 kilometres. These observations were made in July, at a period of meteor activity, when such layers if they exist, would be expected to be enhanced. So far we have not made any observations above 100 kilometres but the April measurements discussed above serve to place an upper limit on the scattering between 60 and 100 kilometres. In the graph in Fig. 20 are plotted Fiocco and Smullins results between 30 and 100 kilometres together with a replot of our results given earlier.

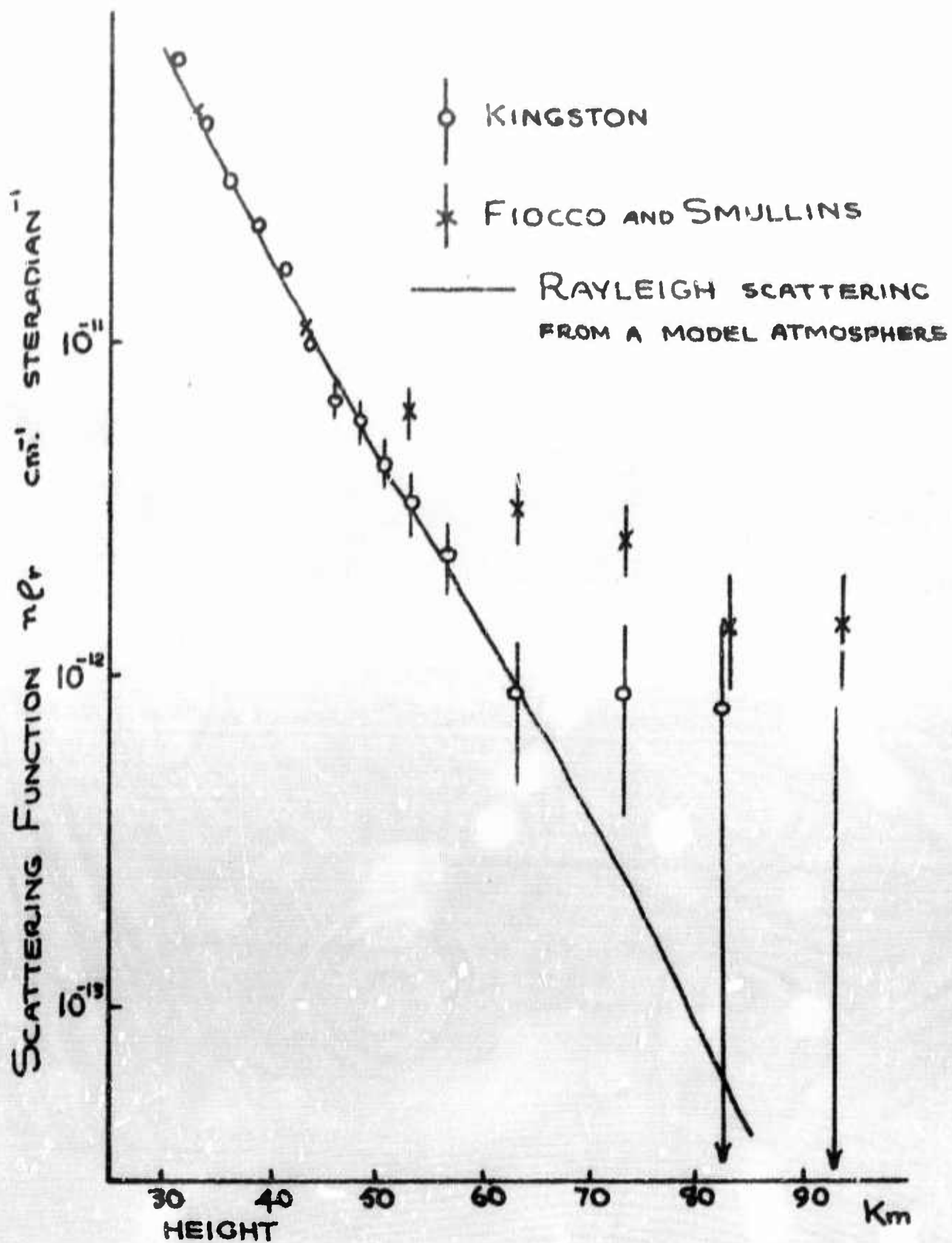


FIG. 20. SCATTERING PROFILES BETWEEN 30 AND 100 KILOMETRES.

Both curves are normalized at a height of 30 kilometres to a scattering function  $np_R$  of  $7.5 \times 10^{-11} \text{ cm}^{-1} \text{ steradian}^{-1}$ , this being the theoretical prediction given in Table I. It can be seen that while both curves agree fairly well over the range 30 - 50 km., where Rayleigh scattering is responsible for both of them, above this height they separate, the scattering at Kingston being on the average a factor of 2.5 less than that obtained by Fiocco and Smullins. The Kingston results, though a little higher than those expected on the basis of Rayleigh scattering from a model atmosphere, do not differ significantly from these. Fiocco and Smullins' results do, and they also differ significantly from those obtained in Kingston.

Two explanations for this difference may be suggested. It is possible that Fiocco and Smullin have some source of extra noise which they have not adequately allowed for, which with our greater sensitivity we have been able to observe and remove. Secondly it may happen that during a period of intense meteor activity the dust layers at these heights have their densities very considerably enhanced. On the results already obtained it is not possible to decide between these two alternatives, and this remains to be one of the first experiments to be carried out during the coming June meteor showers. The possibility also remains that there may be a latitude variation with the concentration of dust increasing with latitude.

#### 4.4 The Daytime Measurements

We have discussed earlier the possibility of daytime measurements and their limitations. Fig.21 shows a graph of  $Ch^2$

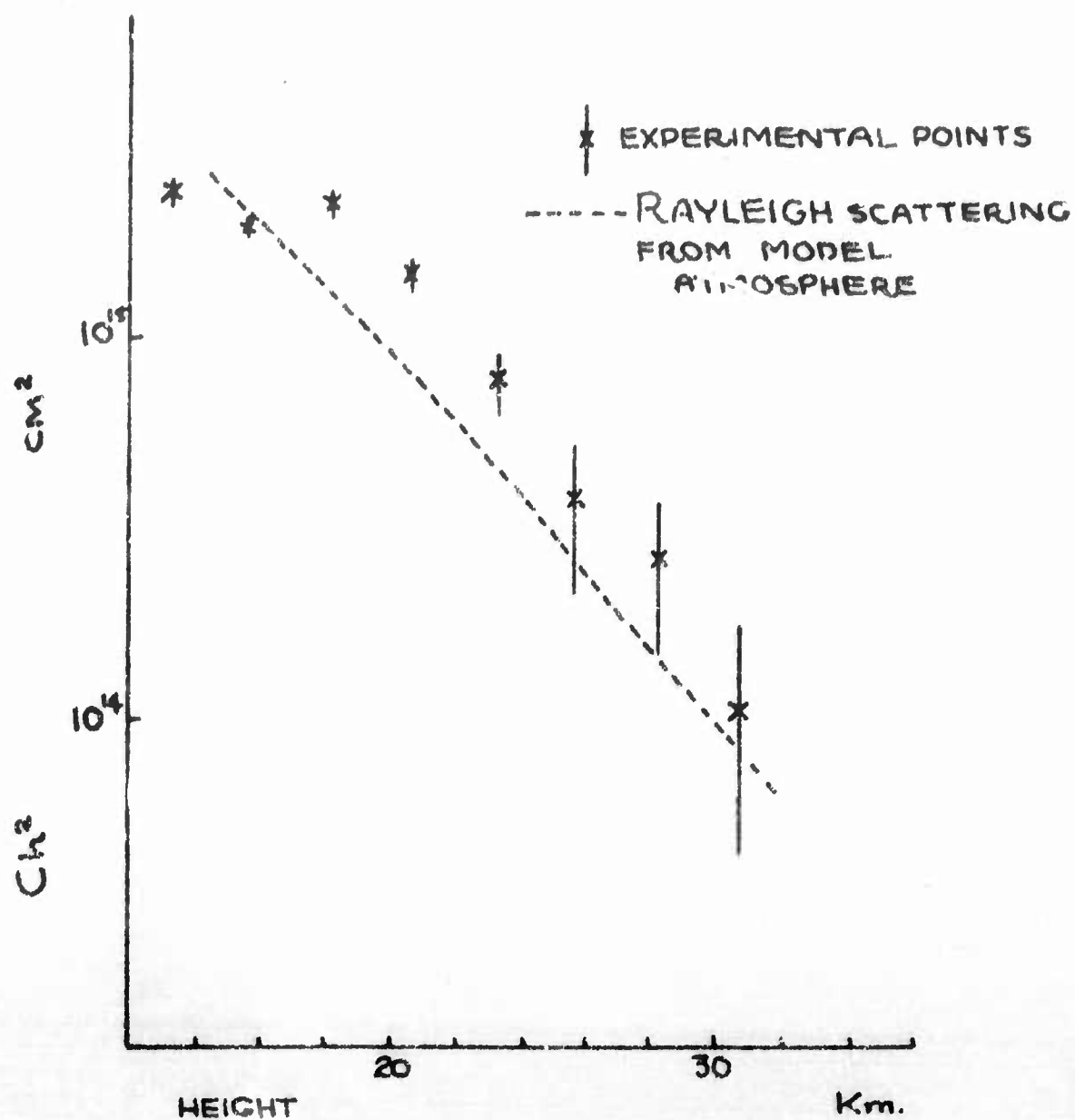


FIG 21 DAYTIME MEASUREMENTS ON THE SCATTERING PROFILE.

versus altitude for a short series of ten shots taken on 16th February. The effect of the background sky noise is very obvious and shows that the limit of present observations is not much greater than 30 kilometres. Below this level however, the profile is very clear, the aerosol layer showing up as well as at night. Very few of these observations have been made yet but it is apparent that, in the absence of cloud, it is possible to obtain a scattering profile up to 30 kilometres at any time of the day or night. As explained earlier a larger transmitting mirror would enable this to be extended upwards by about 10 kilometres.

In the results quoted above, the pulse repetition rate used was one per two minutes as, at that time, there was some uncertainty as to the efficiency of the laser cooling system. Under these circumstances, it took about half an hour to obtain a respectable profile to 30 kilometres. Since then the pulse rate has been increased to two per minute without harm and it seems quite likely that it may be further increased to the equipmental limit of ten per minute. Under these circumstances a profile can be obtained in a few minutes.



## 5. PROGRAMME OF FUTURE WORK

The programme of future work may be divided into two parts, the first of these is the further development of the receiver and transmitter which will be carried on at the same time as the second, which is a series of observations on the various topics discussed in the previous section.

### Development of the Transmitter

There is very little modification which can be usefully done with respect to the transmitter. Tests will clearly have to be made up to its maximum pulse rate but little difficulty is foreseen here. This will involve the installation of a proper refrigeration system to maintain the temperature of the ruby cooling water at a sufficiently low value. At the moment this is cooled by merely placing a vessel containing ice inside the water reservoir.

A larger transmitting mirror of either 32 or 38 cm. diameter will also be installed to enable the daytime measurements to be made to a greater altitude. Experiments may also be made using a passive Q-switch, rather than the existing rotating switch, to obtain a single giant pulse. This will enable better resolution to be made at low altitudes which may be useful in studying the structure of the twenty kilometre aerosol layer.

### Development of the Receiver

The receiver, in contrast to the transmitter, offers considerable scope for improvement. Two main lines of attack are at present being worked on. As mentioned earlier, plans are being made for the



automatic counting of the photomultiplier output. The necessary circuitry for this has been designed and is at present under construction. It is intended to count the photomultiplier output in 63 height-gated ranges, each of length 2 kilometres and with  $\frac{1}{2}$  kilometre dead-space between them. The outputs from the counter will be placed into core storage from which they can be read out onto paper tape and fed directly into an IBM 1620 computer. The use of this device will obviate the necessity for the present tedious analysis of photographic records and enable profiles to be obtained in a very short space of time.

One of the difficulties in the present system is the large dynamic range required in the equipment. This is exemplified in Table 5 where the counting rate varies from about  $10^3$  at a height of 13 kilometres to 0.1 at a height of 60 kilometres. At present, only small height ranges may be examined at a time and these are changed by means of neutral filters. Two possible ways of dealing with this are at the moment under consideration. In the first of these, it is intended to install two additional photomultipliers along with the existing one. Each will receive a different fraction of the signal from the receiving mirror and will be used over a previously selected height range. By careful selection of these ranges it will be possible to make simultaneous observations over the complete range from 10 to 100 kilometres in a way which is not possible at present. The other alternative is to install two new small mirrors each with its own photomultiplier system to look at the lower regions of the atmosphere. Since the signals from low down are strong, these systems could be made very simple, and no

special precautions to differentiate against background noise would be necessary.

The final, and the major, modification to the receiver is to increase the area of the receiving mirror. It was mentioned in Section 2.3 that the quality of this must be such as to resolve the transmitted beam but that it need not be of astronomical quality. Calculations show that a spherical mirror of long focal length and small aperture fulfills the required conditions. It is intended to construct a large parabolic dish consisting of a mosaic of such spherical mirrors, each being perhaps 40 centimetres in diameter. In this way a mirror can be built up of a size which would be prohibitively expensive if cut and ground out of a single piece of glass. Such a dish might consist initially of fifty, 40 centimetre spherical mirrors, given a sensitivity increase of twenty-five over the present arrangement. It will be constructed in such a way that additional mirrors could be added later if required.

#### Future Observations

It is intended to make observations on all the topics discussed in Section 4. and these are listed again here for completeness.

##### i) Variations in Molecular Density

Observations will be made at night on the density of the air between 30 and 70 kilometres. This is a region of considerable theoretical interest as there are large variations in pressure due to atmospheric tides (Haurwitz, 1964). The barometric variations which are only about 0.1% at ground level are believed to increase to

about 10% at an altitude of 100 kilometres. The exact nature of the pressure oscillations, whether they are principally diurnal or semi-diurnal, and the way in which their phase changes with height is still very uncertain. A 10% variation is about at the limit of the sensitivity of our equipment, as it stands at present, at an altitude of 70 kilometres, but it would seem a very worthwhile experiment to attempt to measure these changes. With the future addition of the digital recording equipment it will certainly be possible. It is unfortunate that it is not possible to observe this region during the day, although with the addition of the new transmitting mirror the lowest part of it will be accessible.

ii) The 20 kilometre Aerosol Layer

This has the merit of being accessible twenty-four hours a day and considerable information on it may be obtained using the laser technique. One of the present theoretical problems is its origin. It has been suggested that it may be caused by meteoric dust settling from above; alternatively it may be due to dust carried up from below. Continuous observations of the variations in the layer and their correlation with other meteorological phenomena should enable this to be resolved. Twice daily balloon ascents to altitudes of about 30 kilometres are carried out by the Caribbean Meteorological Service at its station in Kingston. The measurements made during these ascents are available to us through the courtesy of the Director. Further studies of the polarization characteristics should also give information on the nature of the aerosols themselves.



iii) The Upper Dust Layers

Observations during the coming June of the Arietid meteor showers should enable an accurate measurement to be made on the intensity of scatter from these layers. Nightly observations, carried out over a continuous period during and after the meteor showers should give very considerable information both on the meteoric flux rate and the mechanism of disintegration and consequent settling of the particles.

#### REFERENCES

- COLE, A.E. and KANTOR, A.J.      Air Force Interim Supplemental  
atmospheres to 90 Kilometres  
Research Report AFCRL - 63 - 936 (1963)
- DEIRMENDJIAN, D.      Note on Laser Detection of Atmospheric  
Dust Layers.  
J. Geophys. Res. 70: 743-745 (1965)
- ELTERMAN, L.      The Measurement of Stratospheric Density  
Distribution with the Searchlight  
Technique  
J. Geophys. Res. 56: 509-520 (1951)
- ELTERMAN, L.      Seasonal Trends of Temperature, Density,  
and Pressure in the Stratosphere  
Obtained with the Searchlight-Probing  
Technique  
Technical Report AFCRL - 54 - 19 (1954).
- ELTERMAN, L.      Atmospheric Attenuation Model 1964 in  
the Ultraviolet, Visible, and Infrared  
Regions for Altitudes up to 50 km.  
Research Paper AFCRL - 64 - 740 (1964).
- ELTERMAN, L. and CAMPBELL, A.B.      Atmospheric Aerosol Observations with  
Searchlight Probing  
J. Atmos. Sci. 21: 457-458 (1964).
- FIOCCO, G. and COLOMBO, G.      Optical Radar Results and Meteoric  
Fragmentation  
J. Geophys. Res. 69: 1795-1804 (1964).
- FIOCCO, G. and GRAMS, G.      Observations of the Aerosol Layer at 20 km  
by Optical Radar  
J. Atmos. Sci. 21: 323-324 (1964).
- FIOCCO, G. and SMULLIN, L.D.      Detection of Scattering Layers in the  
Upper Atmosphere (60-140 km) by Optical  
Radar.  
Nature 199: 1275-1276 (1963)

- HAURWITZ, B. Tidal Phenomena in the Upper Atmosphere  
Technical Note. WMO -No.146. TP.69.
- HIRONO, M. On the Observation of the Upper Atmospheric Constituents by Laser Beams  
J.Rad.Res.Lab. 11: 251-270 (1964).
- JUNGE, C.E. Air Chemistry and Radioactivity  
Academic Press, (1963).
- JUNGE, C.E., CHAGNON, C.W. and MANSON, J.F. Stratospheric Aerosols  
J. Meteorol. 18: 81-108 (1961).
- JUNGE, C.E. and MANSON, J.E. Stratospheric Aerosol Studies  
J. Geophys. Res. 66: 2163-2182 (1961)
- LONG, R.K. Atmospheric Attenuation of Ruby Lasers  
Proc. Inst. Rad.Eng. 51: 859-860 (1963).
- PALMER, E.P. and ZDUNKOWSKI, W.G. Absolute Scattering Functions and Transmission Values for Interpreting Laser Light Scattering in the Mesosphere.  
J. Geophys. Res. 69: 2369-2377 (1964).
- RAYLEIGH, LORD. Phil. Mag. 51: 107, 274 and 447 (1871).
- ROSEN, J.M. The Vertical Distribution of Dust to 30 Kilometres  
J. Geophys. Res. 69: 4673-4676 (1964).
- VAN DE HULST, H.C. Light Scattering by Small Particles  
John Wiley and Sons. (1957).



Unclassified

Security Classification

DOCUMENT CONTROL DATA - R&D		
(Security classification of title, body of abstract and indexing annotation must be entered when the overall report is classified)		
1. ORIGINATING ACTIVITY (Corporate author) Department of Physics, University of the West Indies, Kingston, Jamaica.		2a. REPORT SECURITY CLASSIFICATION Unclassified
3. REPORT TITLE A Study of the Feasibility of Measuring Atmospheric Densities by using a Laser-Searchlight Technique.		2b. GROUP
4. DESCRIPTIVE NOTES (Type of report and inclusive dates) Annual Scientific Report. April 1st. 1964 - March 31st. 1965.		
5. AUTHOR(S) (Last name, first name, initial) Clemesha, B.R., Kent, I.B., Wright, R.W.H.		
6. REPORT DATE May 1965.	7a. TOTAL NO. OF PAGES 72	7b. NO. OF REFS 10
8a. CONTRACT OR GRANT NO. AP - AROSR - 616-64	8b. ORIGINATOR'S REPORT NUMBER(S) U.W.I. P.S.	
9. PROJECT NO.	9b. OTHER REPORT NO(S) (Any other numbers that may be assigned this report)	
10. AVAILABILITY/LIMITATION NOTICES Qualified requesters may obtain copies of this report from D.D.C.		
11. SUPPLEMENTARY NOTES		12. SPONSORING MILITARY ACTIVITY Hq. AFRL, OAR (UNAF) (CRFP) 1065, Main Street, Waltham, Massachusetts.
13. ABSTRACT An analysis is made of the design of equipment to be used for measuring atmospheric densities by observing the scattering from a laser light-beam projected vertically into the atmosphere. This analysis is made in terms of both the expected scattering under typical conditions and the experimental difficulties which are encountered. A complete description is given of an equipment constructed to make such measurements and the early results are described. It is shown that the method works well with the comparatively simple apparatus used. Up to 30 Km. various dust and aerosol layers can be observed both by day and by night. Between 30 Km. and 70 Km. the variation of the atmospheric density with height can be measured at night and has been found to agree with values calculated on the basis of Rayleigh scattering and assuming a model atmosphere. The possible examination of meteoric dust at altitudes between 80 Km. and 140 Km. is discussed. The proposed future developments of the equipment are outlined.		

DD FORM 1473

Unclassified

Security Classification



Unclassified.  
Security Classification

14 KEY WORDS	LINK A		LINK B		LINK C	
	ROLE	WT	ROLE	WT	ROLE	WT
Atmospheric Density						
Tanors						
Upper Atmosphere						
Aerosols.						

#### INSTRUCTIONS

1. **ORIGINATING ACTIVITY:** Enter the name and address of the contractor, subcontractor, grantee, Department of Defense activity or other organization (corporate author) issuing the report.

2a. **REPORT SECURITY CLASSIFICATION:** Enter the overall security classification of the report. Indicate whether "Restricted Data" is included. Marking is to be in accordance with appropriate security regulations.

2b. **GROUP:** Automatic downgrading is specified in DoD Directive 5200.10 and Armed Forces Industrial Manual. Enter the group number. Also, when applicable, show that optional markings have been used for Group 3 and Group 4 as authorized.

3. **REPORT TITLE:** Enter the complete report title in all capital letters. Titles in all cases should be unclassified. If a meaningful title cannot be selected without classification, show title classification in all capitals in parenthesis immediately following the title.

4. **DESCRIPTIVE NOTES:** If appropriate, enter the type of report, e.g., interim, progress, summary, annual, or final. Give the inclusive dates when a specific reporting period is covered.

5. **AUTHOR(S):** Enter the name(s) of author(s) as shown on or in the report. Enter last name, first name, middle initial. If military, show rank and branch of service. The name of the principal author is an absolute minimum requirement.

6. **REPORT DATE:** Enter the date of the report as day, month, year, or month, year. If more than one date appears on the report, use date of publication.

7a. **TOTAL NUMBER OF PAGES:** The total page count should follow normal pagination procedures, i.e., enter the number of pages containing information.

7b. **NUMBER OF REFERENCES:** Enter the total number of references cited in the report.

8a. **CONTRACT OR GRANT NUMBER:** If appropriate, enter the applicable number of the contract or grant under which the report was written.

8b, 8c, & 8d. **PROJECT NUMBER:** Enter the appropriate military department identification, such as project number, subproject number, system numbers, task number, etc.

9a. **ORIGINATOR'S REPORT NUMBER(S):** Enter the official report number by which the document will be identified and controlled by the originating activity. This number must be unique to this report.

9b. **OTHER REPORT NUMBER(S):** If the report has been assigned any other report numbers (either by the originator or by the sponsor), also enter this number(s).

10. **AVAILABILITY/LIMITATION NOTICES:** Enter any limitations on further dissemination of the report, other than those

imposed by security classification, using standard statements such as:

- (1) "Qualified requesters may obtain copies of this report from DDC."
- (2) "Foreign announcement and dissemination of this report by DDC is not authorized."
- (3) "U. S. Government agencies may obtain copies of this report directly from DDC. Other qualified DDC users shall request through \_\_\_\_\_."
- (4) "U. S. military agencies may obtain copies of this report directly from DDC. Other qualified users shall request through \_\_\_\_\_."
- (5) "All distribution of this report is controlled. Qualified DDC users shall request through \_\_\_\_\_."

If the report has been furnished to the Office of Technical Services, Department of Commerce, for sale to the public, indicate this fact and enter the price, if known.

11. **SUPPLEMENTARY NOTES:** Use for additional explanatory notes.

12. **SPONSORING MILITARY ACTIVITY:** Enter the name of the departmental project office or laboratory sponsoring (paying for) the research and development. Include address.

13. **ABSTRACT:** Enter an abstract giving a brief and factual summary of the document indicative of the report, even though it may also appear elsewhere in the body of the technical report. If additional space is required, a continuation sheet shall be attached.

It is highly desirable that the abstract of classified reports be unclassified. Each paragraph of the abstract shall end with an indication of the military security classification of the information in the paragraph, represented as (TS), (S), (C), or (U).

There is no limitation on the length of the abstract. However, the suggested length is from 150 to 225 words.

14. **KEY WORDS:** Key words are technically meaningful terms or short phrases that characterize a report and may be used as index entries for cataloging the report. Key words must be selected so that no security classification is required. Identifiers, such as equipment model designation, trade name, military project code name, geographic location may be used as key words but will be followed by an indication of technical context. The assignment of links, roles, and weights is optional.